Mycological Progress (2024) 23:9
https://doi.org/10.1007/s11557-024-01947-3

DGfM

ORIGINAL ARTICLE

Xylodon lanatus complex and other additions to *Xylodon*

Eugene Yurchenko[1] · Janett Riebesehl[2] · Ilya Viner[3] · Viviana Motato-Vásquez[4,5] · Otto Miettinen[3]

Received: 14 August 2023 / Revised: 12 December 2023 / Accepted: 31 December 2023

Abstract
Xylodon lanatus and closely related species were studied with molecular and morphological means. This species complex contains six species, two of which we describe as new. Species in the complex have minutely odontioid hymenophore projections that consist of encrusted, firm-walled hyphae and ellipsoid spores. We assign an epitype for *X. lanatus*, for which ITS and 28S rDNA sequences were obtained, and amend the concept of *X. pseudolanatus*. The two new species, both well supported in our phylogenetic analyses, are *X. afromontanus*, found in Eastern Africa, and *X. mantiqueirensis*, found in southeastern Brazil. We show the phylogenetic affinity of *X. echinatus* with *X. lanatus* for the first time, and according to new data the range of the previous species extends to Sunda Archipelago. We provide scanning electron microscopy illustrations of the crystalline deposits on projecting hyphae for the above-mentioned species. The sixth member of the complex is *X. kunmingensis*. Outside the *X. lanatus* complex, we report additional sequenced specimens of *X. hyphodontinus*. A new species, *X. neotropicus* from South America, related to *X. hyphodontinus*, is described. We also describe *X. gloeocystidiifer* from Ecuador as new species. It is characterised by globose/broadly ellipsoid spores, gloeocystidia and capitate cystidia with a resinous cap. The heterotypic names *Hyphodontia yunnanensis* and *Xylodon yunnanensis* are considered. We suggest the previous one is a synonym of the latter.

Keywords *Basidiomycota* · Bayesian phylogram · Corticioid fungi · Crystal morphology · *Hymenochaetales*

Introduction

Xylodon (Pers.) Gray (*Schizoporaceae*, *Hymenochaetales*) is a large genus of corticioid fungi, having cosmopolitan distribution. The concept of this genus, as the main derivative of *Hyphodontia* sensu lato, was proposed by Hjortstam and Ryvarden (2007), and it was emended in subsequent publications, taking into account the results of molecular phylogenetic reconstructions (Riebesehl and Langer 2017; Viner et al. 2018; Riebesehl et al. 2019; Viner et al. 2023). Species of *Xylodon* inhabit dead wood of various sizes, from twigs several mm in diameter to large fallen trunks, and cause white rot. Sometimes basidiomata of *Xylodon* species appear on living parts of trees (Yurchenko 2008) and non-woody plant remains, e.g. fern rachises (Kotiranta and Saarenoksa 2000), herb stems and fallen leaves (Viner et al. 2018), dead polypore basidiomata (Viner et al. 2023). The genus is known from almost all types of world biomes where wooden plant debris occur, from humid to semiarid, and from seashore to upper limit of wooden vegetation in altitudinal gradient.

Riebesehl et al. (2019) showed that *Xylodon* species having minute aculei composed of clustered, projecting, encrusted, more or less firm-walled hyphal ends, belong to at least two groups: the *X. lanatus* species complex (also formulated as *X. lanatus* s. l.) and the *X. hyphodontinus* species complex. The phylogeny of the components of these complexes and some related species were considered in subsequent studies (Wang et al. 2021; Qu et al. 2022).

Section Editor: Yu-Cheng Dai

✉ Janett Riebesehl
janett.riebesehl@julius-kuehn.de

[1] Institute of Forest Sciences, Białystok University of Technology, Wiejska Str. 45A, 15-351 Białystok, Poland

[2] Institute for Plant Protection in Horticulture and Urban Green, Julius Kühn Institute, Messeweg 11/12, DE-38104 Braunschweig, Germany

[3] Finnish Museum of Natural History Luomus, University of Helsinki, P.O. Box 7, FI-00014 Helsinki, Finland

[4] Instituto de Botânica, Núcleo de Pesquisa em Micologia, Av. Miguel Stefano 3687, São Paulo 04301-902, Brazil

[5] Grupo de Investigación en Biología de Microorganismos, Departamento de Biología, Facultad de Ciencias Naturales y Exactas, Universidad del Valle, Calle 13 No. 100-00, Cali, Colombia

Published online: 01 February 2024

In the present work, new phylogeographic and morphological data for *X. lanatus* s. l. and *Xylodon* species with globose to broadly ellipsoid spores and tropical/subtropical distribution (including *X. hyphodontinus*) are considered, and four new species are described.

Material and methods

Morphology study

Specimens stored in herbaria BLS, CFMR, H, KAS, LY, MSK, O, SNP, SP, TNM (acronyms follow Thiers 2023) were examined during this study. Some specimens were duplicated, which is noted by 'dupl.' abbreviation before the herbarium acronym.

Macromorphology was studied on dried specimens. For micromorphology studies, slides of basidiomata sections prepared manually in 3% aqueous solution of potassium hydroxide (abbreviated as KOH), were used. Additional preparations were done in Melzer's reagent (abbreviated as Mz) to study incrustations on hymenial elements and hyphae, and to test spore amyloid/dextrinoid reaction. In case of absence of both types of reaction, the abbreviation 'Mz−' is used in protologues. Cyanophily of spores was examined in 0.02% cotton blue in 50% aqueous lactic acid (abbreviated as CB). Measurements of microstructures were done on a Nikon Eclipse Ni-U light microscope (Nikon Corp., Japan) by NIS-Elements Br imaging software (Nikon Corp.), mostly under ×1000 magnification. Mean spore length (L) and width (W) were calculated as arithmetic averages for 30 spores, randomly selected in squash preparations in KOH. Spore quotient (Q) was determined as length/width ratio for individual spores. Hymenophoral aculei density was measured by overlaying a scale line 1 mm long on photographs in 5 occasional places and calculating the number of aculei crossed by this line.

Scanning electron microscopy (SEM) studies were performed on a desktop microscope Phenom G2 pro (Labmate, UK). For this, pieces of basidiomata about 2×2 mm, taken from herbarium, were attached by double sided carbon adhesive discs (Leit tabs) to aluminium pin stubs, coated with 5–6 nm thick layer of gold in a Leica EN ACE200 vacuum sputter (Leica Microsystems, Germany), and examined at magnifications ×4100…×15500.

DNA extraction, amplification and sequencing

DNA was extracted from pieces of dried basidiomata 4−16 mm^2 in size with E.Z.N.A.® Fungal DNA Mini Kit (Omega Bio-Tek, VWR, Radnor, Pennsylvania, USA) following manufacturer's instructions. These pieces were cut in the way to minimise the amount of substratum in the sample. For a part of specimens, total genomic DNA was extracted from dried fungi using a CTAB-chloroform extraction protocol (Kutuzova et al. 2017).

Nuclear ribosomal DNA ITS region, including ITS1, 5.8S RNA gene, and ITS2, were amplified with different combinations of primers ITS1F (Gardes and Bruns 1993), ITS1, ITS2, ITS3, ITS4, ITS5 (White et al. 1990), 58A1F (Martin and Rygiewicz 2005), LR22 (https://sites.duke.edu/vilgalyslab/files/2017/08/rDNA-primers-for-fungi.pdf) and ALR0.2 (Riebesehl and Langer 2017). The beginning D1-D2 domains of 28S rRNA gene were amplified with primers LR0R (Bunyard et al. 1996), LR5 (Vilgalys and Hester 1990), LR7 (Hopple and Vilgalys 1994), NL1, NL4 (O'Donnell 1993) and JS1 (Landvik 1996).

PCR products were purified with a DNA Clean & Concentrator®-5 kit (Zymo Research, Irvine, California, USA), then sequenced by LGC Genomics GmbH (Berlin, Germany). For some specimens, PCR products were purified from agarose gels using a Fermentas Genomic DNA Purification Kit (ThermoFisher Scientific, Waltham, Massachusetts); sequencing reactions were performed on an ABI 3730XL DNA analyzer (Applied Biosystems) by Macrogen (Amsterdam, the Netherlands).

The sequences were edited and assembled with MEGA11 (Tamura et al. 2021). Five quality check guidelines (Nilsson et al. 2012) were applied to them, after which sequences were deposited in NCBI GenBank (Benson et al. 2018, https://www.ncbi.nlm.nih.gov/genbank). Sequences, generated in this study, are listed in Table 1.

Phylogenetic analysis

Additional sequences were downloaded from NCBI GenBank (Tab. 1). We collected in the datasets the available sequences of all *Xylodon* species (at least one representative for every species) represented in the database. *Lyomyces sambuci*, the type species of the closely related genus *Lyomyces,* was assigned as the outgroup for phylograms. The smaller subset, including the members of *X. lanatus* complex only, was composed to save more informative position for Maximum Likelihood (ML) calculations. Mid-point rooting was applied to the phylogram based on this smaller dataset. Datasets were created with MEGA11 and alignments were calculated with MAFFT v. 7 (Katoh et al. 2019; https://mafft.cbrc.jp/alignment/server), using L-INS-i algorithm for ITS and G-INS-i for 28S dataset. Bayesian inference of the phylogeny (BI) and ML method were used for tree building. Sequence alignments are available as supplementary material to this article. Dissimilarities between selected sequences were calculated by computing pairwise distances in MEGA11.

BI phylograms were computed with TrEase (Mishra et al., http://www.thines-lab.senckenberg.de/trease) using MrBayes v. 3.2 (Ronquist et al. 2012), using substitution

Table 1 Sequences used for phylogenetic reconstructions*

Species	Specimen voucher	GenBank accession number		Country	Reference
		ITS	28S		
Hyphodontia yunnanensis C.L. Zhao & Y.C. Dai	CLZhao 6804 (SWFC), holotype	MW020702		China	Boonmee et al. 2021
Lyomyces sambuci (Pers.) P. Karst.	KAS-JR7	KY800402	KY795966	Germany	Yurchenko et al. 2017
Xylodon acuminatus Viner & K.H. Larss.	KHL 16029 (GB-0207638), holotype	ON197552	ON197552	Brazil	Viner et al. 2023
X. acystidiatus Xue W. Wang & L.W. Zhou	LWZ 20180514-9 (MEL), holotype	MT319474	MT319211	Australia	Wang et al. 2021
X. afromontanus Yurchenko & Viner	**O-F-904012, holotype**	**OQ645463**		**Rwanda**	**This study**
X. angustisporus Viner & Ryvarden	LR 50691b (O), holotype	OK273831	OK273831	Cameroon	Viner et al. 2021
X. apacheriensis (Gilb. & Canf.) Hjortstam & Ryvarden	Canfield 180 (BPI), holotype	KY081800		USA, Arizona	Riebesehl and Langer 2017
	Miettinen 16686 (H)		OK273835	USA, Texas	Viner et al. 2021
X. asperus (Fr.) Hjortstam & Ryvarden	Spirin 11923 (H)	OK273838	OK273838	Russia	Viner et al. 2021
X. astrocystidiatus (Yurchenko & Sheng H. Wu) Riebesehl, Yurchenko & E. Langer	Wu 9211-71 (TNM F24764), holotype	NR154054	NG068732	Taiwan	Yurchenko and Wu 2014
X. attenuatus Spirin & Viner	Spirin 8775 (H), holotype	NR173787		USA, Washington	Viner et al. 2018
	Spirin 8714 (H)		OK273839	USA, Washington	Viner et al. 2021
X. australis (Berk.) Hjortstam & Ryvarden	LWZ 20180513-6 (HMAS), epitype	MT319505	MT319249	Australia	Wang et al. 2021
X. bambusinus C.L. Zhao & X. Ma	CLZhao 11310 (SWFC), holotype	MW394660	MW394655	China	Ma and Zhao 2021
X. borealis (Kotir. & Saaren.) Hjortstam & Ryvarden	Spirin 10911 (H)	OK273846	OK273846	Russia	Viner et al. 2021
X. brevisetus (P. Karst.) Hjortstam & Ryvarden	UC2023199	KP814485		Canada, British Columbia	Rosenthal et al. 2017
	JS17863 (O)		AY586676	Norway	Larsson et al. 2004
X. crystalliger Viner	KUN 2312 (H), holotype	NR166242		Russia	Viner et al. 2018
	KUN 3347 (H)		OK273842	Russia	Viner et al. 2021
X. cymosus (D.P. Rogers & H.S. Jacks.) Viner & Miettinen	Miettinen 19606 (H 7200259)	ON197554		USA, North Carolina	Viner et al. 2023
X. cystidiatus (A. David & Rajchenb.) Riebesehl & E. Langer	AS171128/1625B (TUF)	OK273850	OK273850	Kenya	Viner et al. 2021
X. damansaraensis Xue W. Wang & L.W. Zhou	LWZ 20180417-20 (HMAS), holotype	MT319497	MT319242	Malaysia	Wang et al. 2021
X. daweishanensis C.L. Zhao	CLZhao 18357 (SWFC), holotype	OP730715		China	Guan et al. 2023
	CLZhao 18446 (SWFC)		OP730725	China	Guan et al. 2023
X. detriticus (Bourdot) K.H. Larss., Viner & Spirin	Miettinen 22106 (H)	OK273844	OK273844	Portugal	Viner et al. 2021
X. dissiliens Viner & Ryvarden	LR 44817 (O), holotype	OK273856	OK273856	Uganda	Viner et al. 2021

Table 1 (continued)

Species	Specimen voucher	GenBank accession number		Country	Reference
		ITS	28S		
X. echinatus (Yurchenko & Sheng H. Wu) Riebesehl, Yurchenko & E. Langer	**KAS-JR31**	**OQ645466**	**OQ645484**	**Malaysia, Sabah**	**This study**
	OM 16459 (H 7200689)	**OQ645465**		**Malaysia, Sabah**	**This study**
	OM 18328 (H 7200350)	**OQ645464**		**Indonesia, Jawa Tengah**	**This study**
X. filicinus Yurchenko & Riebesehl	MSK-F 12869, holotype	MH880199	NG067836	Taiwan	Riebesehl et al. 2019
X. fissuratus C.L. Zhao	CLZhao 9407 (SWFC), holotype	OP730714		China	Guan et al. 2023
X. flaviporus (Berk. & M.A. Curtis ex Cooke) Riebesehl & E. Langer	FR-0249797	MH880201	MH884901	Réunion	Riebesehl et al. 2019
X. flocculosus C.L. Zhao	CLZhao 18342 (SWFC), holotype	MW980776	MW980779	China	Qu and Zhao 2022
X. follis Riebesehl, Yurchenko & E. Langer	FR-0249814, holotype	MH880204	NG153866	Réunion	Riebesehl et al. 2019
X. gloeocystidiifer Yurchenko & Riebesehl	**EYu 190721-61 (BLS M-5232), holotype**	**OQ645467**	**OQ645485**	**Ecuador**	**This study**
	EYu 190720-11 (CFMR)	**OR240822**		**Ecuador**	**This study**
X. gossypinus C.L. Zhao & K.Y. Luo	CLZhao 8375 (SWFC), holotype	MZ663804	MZ663813	China	Luo et al. 2021
X. grandineus K.Y. Luo & C.L. Zhao	CLZhao 6425 (SWFC), holotype	OM338090	OM338099	China	Luo et al. 2022
X. hastifer (Hjortstam & Ryvarden) Hjortstam & Ryvarden	LR 19767 (K), holotype	KY081801		Argentina	Riebesehl and Langer 2017
X. heterocystidiatus (H.X. Xiong, Y.C. Dai & Sheng H. Wu) Riebesehl, Yurchenko & E. Langer	Wu 9209-27 (TNM F24726)	JX175045		Taiwan	Yurchenko and Wu 2014
	Wu 9209-27 (TNM F24726)		KX857821	Taiwan	unpublished
X. hjortstamii (Gresl. & Rajchenb.) Riebesehl & E. Langer	Gorjón 3187 (GB)	ON188816	ON188816	Chile	Viner et al. 2023
X. hyphodontinus (Hjortstam & Ryvarden) Riebesehl, Yurchenko & G. Gruhn	AS171124/1235 (H 7008787)	OK273848	OK273848	Kenya	Viner et al. 2021
	KAS-GEL9222	MH880205	MH884903	Kenya	Riebesehl et al. 2019
	O-F-907725	**OQ992549**		**Cameroon**	**This study**
	EYu 190728-2 (MSK-F 11103)	**OQ645469**	**OQ645487**	**Panama**	**This study**
	EYu 190728-9 (BLS M-5237)	**OQ645470**	**OQ645488**	**Panama**	**This study**
	EYu 190720-68 (BLS M-5236)	**OQ645471**	**OQ645489**	**Ecuador**	**This study**
	EYu 110623-23b (MSK-F 7397)	**OQ645468**	**OQ645486**	**Taiwan**	**This study**
	LR 12558 (KAS)	MH880209		Spain, La Gomera	Riebesehl et al. 2019
	LIP GG-GUY13-044	MH880206	MH884904	French Guiana	Riebesehl et al. 2019
	LIP GG-MAR12-238	MH880207	MH884905	Martinique	Riebesehl et al. 2019
	LIP GG-MAR15-127	MH880208	MH884906	Martinique	Riebesehl et al. 2019
X. kunmingensis L.W. Zhou & C.L. Zhao	CLZhao 3019 (SWFC), holotype	MW404532		China	Shi et al. 2019
	LWZ 20170820-41 (IFP)	MT319512		China	Wang et al. 2021

Table 1 (continued)

Species	Specimen voucher	GenBank accession number		Country	Reference
		ITS	28S		
	SFC 20170317-07	MZ520580		South Korea	Cho et al. 2021
	MSK-F 7381	MH880196		Taiwan	Riebesehl et al. 2019
	TUB-FO 42450	MH880197		Taiwan	Riebesehl et al. 2019
	TUB-FO 42565	MH880198	MH884898	Taiwan	Riebesehl et al. 2019
X. laceratus C.L. Zhao	CLZhao 9892 (SWFC), holotype	OL619258		China	Qu et al. 2021
	CLZhao 9841 (SWFC)		OL619265	China	Qu et al. 2021
X. lagenicystidiatus Xue W. Wang & L.W. Zhou	LWZ 20180513-16 (MEL), holotype	MT319634	MT319368	Australia	Wang et al. 2021
X. lanatus (Burds. & Nakasone) Hjortstam & Ryvarden	**OM 17683 (H 7200691)**	**OQ645473**		**USA, North Carolina**	**This study**
	FP-101864-A (CFMR)	**OQ645474**	**OQ645490**	**USA, Mississippi**	**This study**
	OM 17835.3 (H 7200692)	**OQ645472**		**USA, Florida**	**This study**
	FP-102919-Sp (CFMR)	**OQ645475**	**OQ645491**	**USA, Puerto Rico**	**This study**
	KAS-Ec720	**OQ645476**		**Ecuador**	**This study**
X. laxiusculus Viner & Ryvarden	LR 44877 (O), holotype	OK273827		Uganda	Viner et al. 2021
X. lenis Hjortstam & Ryvarden	Wu 0808-32 (TNM F22659)	JX175043		Taiwan	Yurchenko and Wu 2014
	Wu 0808-32 (TNM F22659)		KX857820	Taiwan	Chen et al. 2017
X. macrosporus C.L. Zhao & K.Y. Luo	CLZhao 10226 (SWFC), holotype	MZ663809	MZ663817	China	Luo et al. 2021
X. magallanesii Fernández-López, Telleria, M. Dueñas, M. Laguna & M.P. Martín	MA-Fungi 90397, holotype	MT158729	NG075344	Chile, Los Lagos	Fernández-López et al. 2020
X. magnificus (Gresl. & Rajchenb.) K.H. Larss.	**HHB-18010 (CFMR)**		**MK598742**	**New Zealand, Campbell Island**	**This study**
X. mantiqueirensis Yurchenko, Motato-Vásq. & Viner	**MV529 (SP467059), holotype**	**OQ645478**		**Brazil, São Paulo**	**This study**
	MV509 (SP498989)	**OQ645477**		**Brazil, São Paulo**	**This study**
X. mollissimus (L.W. Zhou) C.C. Chen & Sheng H. Wu	Miettinen 12791.1 (H)	ON188815	ON188815	Indonesia	Viner et al. 2023
X. montanus C.L. Zhao	CLZhao 8179 (SWFC), holotype	OL619260	OL619268	China	Qu et al. 2021
X. neotropicus Yurchenko, Motato-Vásq. & Viner	**MV580 (SP467086), holotype**	**OQ645479**	**OQ645479**	**Brazil, Rio de Janeiro**	**This study**
	EYu 190721-12a (BLS M-5235)	**OQ645480**	**OQ645492**	**Ecuador**	**This study**
	EYu 190721-12b (BLS M-5234)	**OQ645481**	**OQ645493**	**Ecuador**	**This study**
X. nesporii (Bres.) Hjortstam & Ryvarden	Viner 2019_59 (H)	OK273834	OK273834	Russia	Viner et al. 2021
X. niemelaei (Sheng H. Wu) Hjortstam & Ryvarden	TU114922	OK273836	OK273836	Réunion	Viner et al. 2021
X. nongravis (Lloyd) C.C. Chen & Sheng H. Wu	Spirin 5615 (H)	OK273849	OK273849	Russia	Viner et al. 2021
X. nothofagi (G. Cunn.) Hjortstam & Ryvarden	PDD 91630	GQ411524		New Zealand	Fukami et al. 2010
	ICMP 13839		MH260064	New Zealand	Fernández-López et al. 2018

Table 1 (continued)

Species	Specimen voucher	GenBank accession number		Country	Reference
		ITS	28S		
X. ovisporus (Corner) Riebesehl & E. Langer	KAS-GEL3493	EU583421		Taiwan	Yurchenko et al. 2020
	ICMP 13835		MH260063	Taiwan	Fernández-López et al. 2018
X. paradoxus (Schrad.) Chevall.	Oivanen PO109 (H 6111044)	OK273843	OK273843	Finland	Viner et al. 2021
X. pruinosus (Bres.) Spirin & Viner	Viner 2019_21 (H)		OK273845	Finland	Viner et al. 2021
X. pruniaceus (Hjortstam & Ryvarden) Hjortstam & Ryvarden	LR 11251 (O)	OK273828		Malawi	Viner et al. 2021
X. pseudolanatus Nakasone, Yurchenko & Riebesehl	FP-150922 (CFMR), holotype	MH880220	MH884090	Belize	Riebesehl et al. 2019
	HHB-10703-Sp (CFMR)	OK273847	OK273847	USA, Virginia	Viner et al. 2021
	HHB-4305 (CFMR)	**OQ645482**		**USA, Tennessee**	**This study**
	OM 17556.2 (H 7200690)	**OQ645483**		**USA, North Carolina**	**This study**
X. pseudotropicus (C.L. Zhao, B.K. Cui & Y.C. Dai) Riebesehl, Yurchenko & E. Langer	Dai 10768 (BJFC), holotype	KF917543		China	Zhao et al. 2014
	Dai 16167 (BJFC)		MT319255		Wang et al. 2021
	LWZ 20170817-1 (IFP)	MT319507			Wang et al. 2021
	Miettinen 16558.2 (H)	OK273854		Malaysia	Viner et al. 2021
X. puerensis C.L. Zhao	CLZhao 8142 (SWFC), holotype	OP730720	OP730728	China	Guan et al. 2023
X. quercinus (Pers.) Gray	Spirin 12030 (H)	OK273841	OK273841	Russia	Viner et al. 2021
X. raduloides Riebesehl & E. Langer	Dai 12631 (BJFC)	KT203307	KT203328		unpublished
X. ramicida Spirin & Miettinen	Spirin 7670 (H)	ON188817	ON188817	Russia	Viner et al. 2023
X. rhododendricola Xue W. Wang & L.W. Zhou	LWZ 20180512-4 (MEL), holotype	MT319619	MT319355	Australia	Wang et al. 2021
X. rimosissimus (Peck) Hjortstam & Ryvarden	Miettinen 12026.1 (H)	OK273840	OK273840	Norway	Viner et al. 2021
X. serpentiformis (E. Langer) Hjortstam & Ryvarden	KAS-GEL3668	MH880227		Taiwan	Riebesehl et al. 2019
	LWZ 20170818-4 (IFP)		MT319213		Wang et al. 2021
X. sinensis C.L. Zhao & K.Y. Luo	CLZhao 11120 (SWFC), holotype	OK560885	MZ663819	China	Luo et al. 2021
X. spathulatus (Schrad.) Kuntze	MSK-F 12931	MH880231	MH884914	Russia	Riebesehl et al. 2019
X. subclavatus (Yurchenko, H.X. Xiong & Sheng H. Wu) Riebesehl, Yurchenko & E. Langer	TUB-FO 42167	MH880232		Taiwan	Riebesehl et al. 2019
X. subflaviporus C.C. Chen & Sheng H. Wu	Wu 0809-76 (TNM F29958), holotype	NR184880	NG068781	China	Chen et al. 2017
X. submucronatus (Hjortstam & Renvall) Hjortstam & Ryvarden	Renvall 1602 (H), holotype	OK273830		Tanzania	Viner et al. 2021
X. subserpentiformis Xue W. Wang & L.W. Zhou	LWZ 20180513-28 (MEL), holotype	MT319480	MT319222	Australia	Wang et al. 2021
X. subtilissimus Viner & Spirin	Spirin 12228 (H 7074041), holotype	ON188818	ON188818	Russia	Viner et al. 2023

Table 1 (continued)

Species	Specimen voucher	GenBank accession number		Country	Reference
		ITS	28S		
X. subtropicus (C.C. Chen & Sheng H. Wu) C.C. Chen & Sheng H. Wu	Wu 9806-105 (TNM F8988)	KX857807	KX857809	Vietnam	Chen et al. 2017
X. tropicus C.L. Zhao	CLZhao 3351 (SWFC), holotype	OL619261	OL619269	China	Qu et al. 2022
X. ussuriensis Viner	KUN 1989 (H), holotype	NR166241		Russia	Viner et al. 2018
X. verecundus (G. Cunn.) Yurchenko & Riebesehl	KHL 12261 (GB)	DQ873642	DQ873643	USA	Larsson et al. 2006
X. victoriensis Xue W. Wang & L.W. Zhou	LWZ 20180512-11 (MEL), holotype	MT319485	MT319227	Australia	Wang et al. 2021
X. wenshanensis K.Y. Luo & C.L. Zhao	CLZhao 15729 (SWFC), holotype	OM338097	OM338104	China	Luo et al. 2022
X. xinpingensis C.L. Zhao & X. Ma	CLZhao 9174 (SWFC), holotype	MW394657	MW394650	China	Ma and Zhao 2021
X. yarraensis Xue W. Wang & L.W. Zhou	LWZ 20180509-7 (MEL), holotype	MT319640	MT319371	Australia	Wang et al. 2021
X. yunnanensis Xue W. Wang & L.W. Zhou	LWZ 20180920-12a (HMAS), holotype	MT319651	MT319252	China	Wang et al. 2021

*New sequences are shown in bold

models suggested by TOPALi v. 2.5 (Milne et al. 2008) and based on Akaike information criterion (AIC), one million generations, with a burn-in of 25% of trees to discard, and other parameters as default. FigTree v. 1.4.4 (Rambaut 2018; http://tree.bio.ed.ac.uk/software/figtree) was used for processing the BI phylograms. ML phylograms were calculated with MEGA11 under usage of substitution models based on AIC, suggested also by TOPALi v. 2.5. Bootstrap replications of 1000, and other settings as default were applied. Final versions of the phylograms were prepared in CorelDRAW v. 9 (Corel Corp., Ottawa, Canada, 1999).

Results

Phylogeny

Twenty-three ITS sequences from eight species and twelve 28S sequences from six species were generated in our study. The sequences of *Xylodon lanatus* s. str. (ITS and 28S), *X. echinatus* (ITS and 28S), and *X. magnificus* (28S) were obtained for the first time from these species. The oldest herbarium specimens from which ITS sequences of good quality were obtained, were 48 and 46 years old at the time of DNA extracting (CFMR HHB-4305, collected in 1970; O-F-904012, collected in 1974, respectively).

The final aligned ITS datamatrix consisted of 101 taxa and 824 positions. Some positions were manually adjusted based on their presumed homology, and where the L-INS-i algorithm did not result in optimal alignment. Also, some supposedly nonalignable positions were manually removed from the dataset. GTR+G model was suggested for BI and ML by TOPALi v. 2.5. Subsequently, model 6 (GTR) was chosen for the BI calculations with TrEase and GTR+G for the ML calculations with MEGA11.

The smaller aligned datamatrix, including the species related to *X. lanatus* only, consisted of 17 taxa and 667 positions. GTR+G model was suggested for BI and ML by TOPALi v. 2.5 for this dataset. Then model 6 (GTR) was chosen for BI calculations in TrEase, and GTR+G for ML calculations in MEGA11.

The final 28S alignment consisted of 81 taxa and 939 positions. GTR+I+G model was suggested for BI and ML by TOPALi v. 2.5. Subsequently, model 6 (GTR) was chosen for the BI calculations with TrEase and GTR+I+G for the ML calculations with MEGA11.

A high degree of agreement between BI and ML trees was observed for terminal clades, but deeper branching showed limited congruence (Figs. 1, 2, 4).

The phylogeny revealed six distinct subclades in the *X. lanatus* species complex (all with PP = 1): (1) *X. lanatus* s. str.; (2) *X. pseudolanatus*; (3) *X. kunmingensis*; (4) *X. mantiqueirensis*; (5) *X. echinatus*; (6) *X. afromontanus*, based on a single specimen (Figs. 2, 3). ITS sequences of *X. pseudolanatus* demonstrate a high homogeneity: no more than 0.36% of dissimilarity. The maximum dissimilarity between ITS sequences in cluster *X. lanatus* s. str. reaches 1.45%. The subclades *X. lanatus* s. str., *X. pseudolanatus*,

X. kunmingensis and *X. echinatus* are well distinguished in the 28S-based phylogeny too (Fig. 4). A specimen CFMR HHB-4305, treated earlier as paratype of *X. lanatus* s. str. (Riebesehl et al. 2019), after this phylogenetic study was belonged to *X. pseudolanatus*.

The ITS sequences of *X. echinatus*, derived from specimens collected in Borneo (KAS-JR31) and Java (H 7200350), have differences in 5 positions (0.85%). This study confirms that *X. echinatus* belongs to the *X. lanatus* species complex, as it was suggested earlier from the morphology (Riebesehl et al. 2019). Before the publication of *X. echinatus* (Yurchenko et al. 2013), S.H. Wu and co-workers failed to obtain sequences from the type material. Our attempts to obtain sequences from the holotype (TNM F24751) were also unsuccessful.

Our study contributed four new sequences to *X. hyphodontinus* (BLS M-5236, BLS M-5237; MSK-F 7397, MSK-F 11103), which grouped in a strongly supported clade (PP = 1) together with seven sequences, published earlier (Fig. 2). This clade demonstrates five phylogenetically distinct subclades in both phylogenies (Figs. 2, 4). Additionally, we obtained ITS2 sequence for *X. hyphodontinus* from Cameroon (O-F-907725). It is identical to the sequences of this segment for *X. hyphodontinus* from Kenya: there is a difference in a single bp between O-F-907725 and KAS-GEL9222, and no differences between O-F-907725 and H 7008787.

Three newly obtained sequences from South America form a well-supported clade (PP = 1), named here *X. neotropicus*. Two of them (BLS M-5233, BLS M-5234) originate from the same locality and one substratum unit in Ecuador, whereas SP467086 originates from Brazil. There are differences in 7 positions (including using the ambiguity code twice in BLS M-5234) between the ITS sequences of BLS M-5233 and BLS M-5234, and we suppose that these sequences were obtained from two genetically different, but neighbouring fungal individuals. NCBI BLAST for BLS M-5234 suggested *X. hyphodontinus* LR 12558 (91.02% similarity) and *X. hastifer* LR 19767 (88.94% similarity) as the most similar ITS sequences. The phylogenetic reconstructions (Figs. 2 and 4) demonstrated that *X. neotropicus* belong to the same clade as *X. hyphodontinus* (PP = 1).

The phylograms (Figs. 2 and 4) demonstrate that two sequences, called *X. gloeocystidiifer*, belong to the same clade (PP = 1) as *X. hyphodontinus* and *X. neotropicus*. NCBI BLAST suggested *X. tropicus* CLZhao 3397 (86.51% similarity) and *X. ramicida* Spirin 7670 (86.36% similarity) as the most similar ITS sequences for *X. gloeocystidiifer* BLS M-5232.

The inclusion of 28S rRNA gene barcode of a specimen collected from New Zealand and identified as *X. magnificus* in our phylogenetic reconstruction confirmed that this species is related to *X. pruinosus* and *X. detriticus* (Fig. 4) as suggested by Viner et al. (2018). All three taxa were previously classified in *Lagarobasidium*.

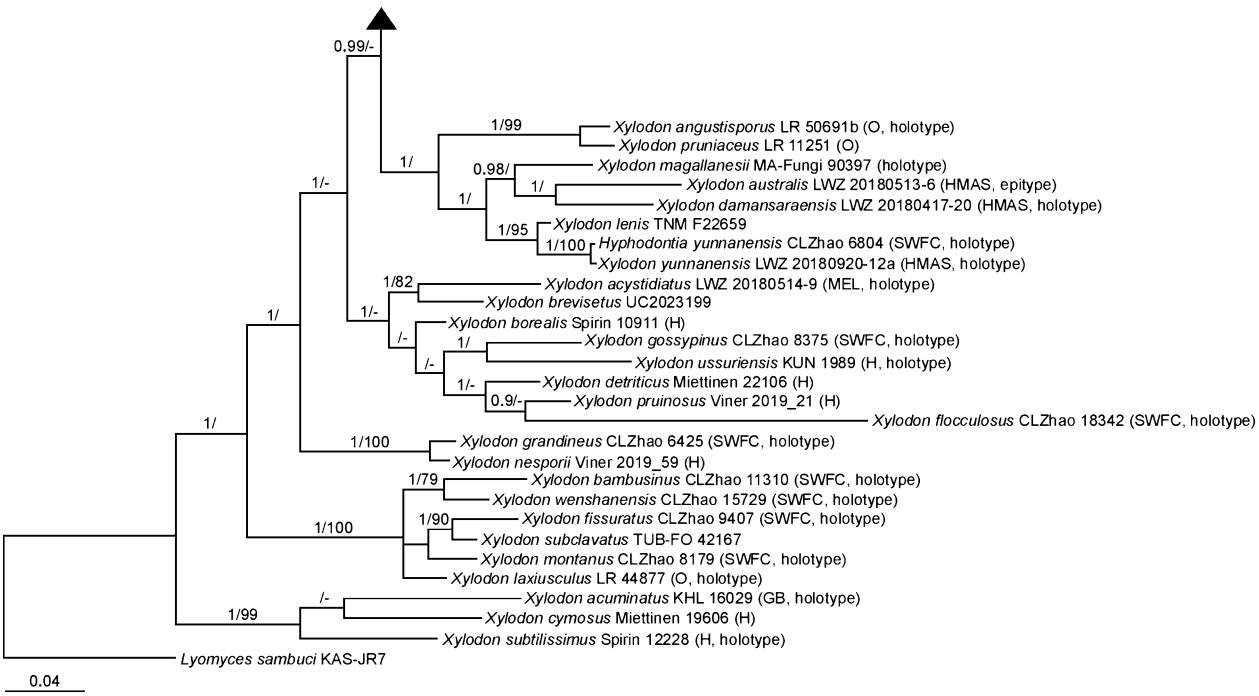

Fig. 1 Bayesian inference of phylogeny of *Xylodon* species based on ITS sequences. Sequences obtained in this study are given in bold. The numbers above branches denote posterior probability (PP≥0.9) values for BI / bootstrap support (BS>75%) in ML phylogram; '-' means the absence of the branch in ML phylogram. Scale bar shows the number of substitutions per site

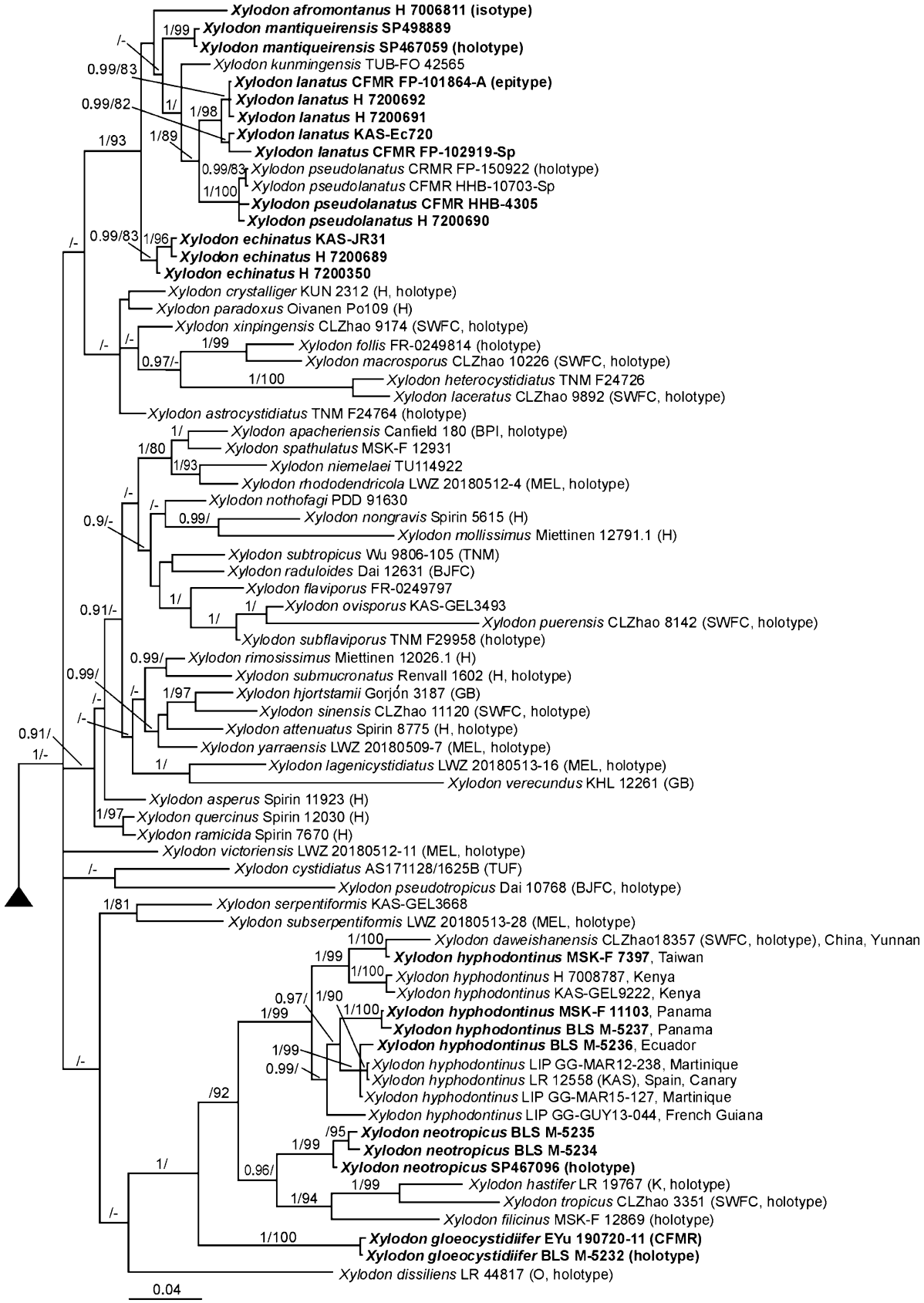

Fig. 2 Continuing of the phylogram from Fig. 1

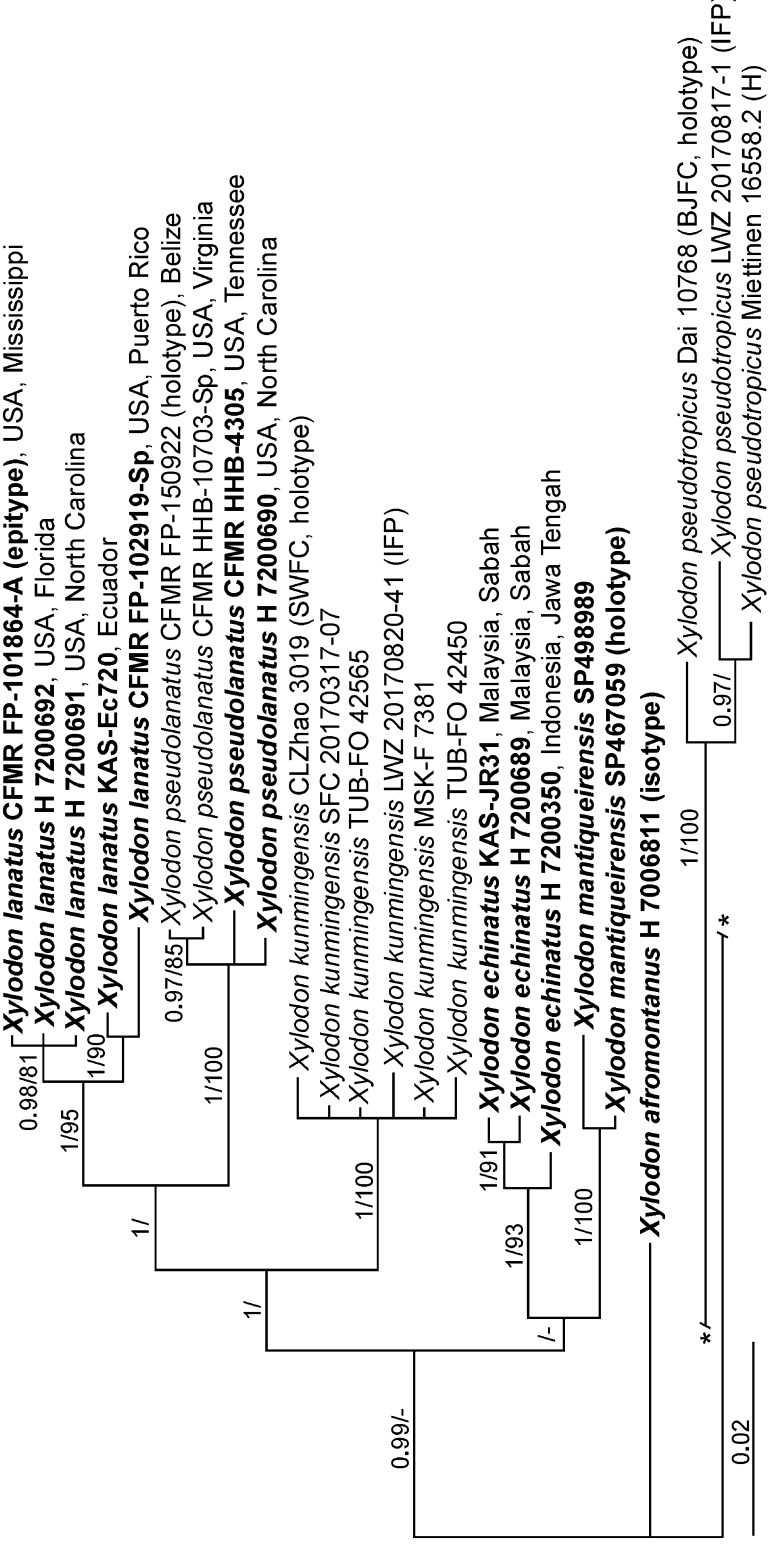

Fig. 3 Bayesian inference of phylogeny of *Xylodon lanatus* species complex based on ITS sequences. Sequences obtained in this study are given in bold. The numbers above branches denote posterior probability (PP≥0.9) values for BI/bootstrap support (BS>75%) in ML phylogram; '-' means the absence of the branch in ML phylogram. Scale bar shows the number of substitutions per site

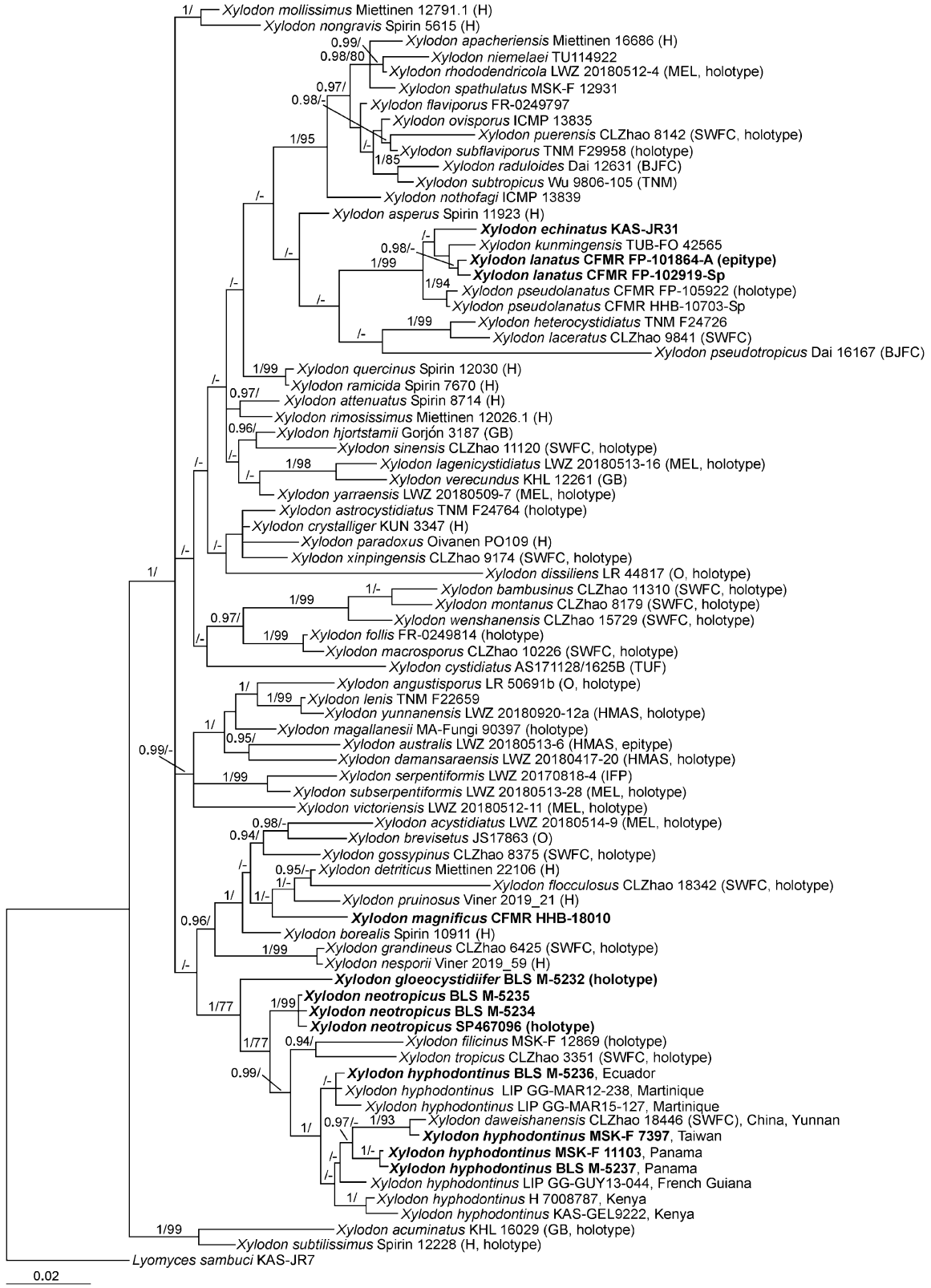

Fig. 4 Bayesian inference of phylogeny of *Xylodon* species based on 28S sequences. Sequences obtained in this study are given in bold. The numbers above branches denote posterior probability (PP≥0.9) values for BI / bootstrap support (BS>75%) in ML phylogram; '-' means the absence of the branch in ML phylogram. Scale bar shows the number of substitutions per site

Morphology

The complex phylogenetic structure of *X. lanatus* s. l., observed in our study, opened the questions how to treat the subclades within this complex in terms of morphology. At the same time, the attempts to obtain DNA barcodes from *X. lanatus* holotype (CFMR HHB-8925) by Riebesehl et al. (2019) were not successful. To understand better the taxa within *X. lanatus* s. l., both in terms of morphology and molecular phylogeny, we introduce here an epitype for *X. lanatus*, supported by sequence data. The selected epitype was collected close to the *locus classicus*, though 5 years later than the holotype, and from a similar kind of substratum. The epi- and holotype are morphologically highly similar. The description of *X. lanatus* s. str., based on the three specimens from continental North America, is given below. The exclusion of two specimens of *X. lanatus*, collected in tropical areas, is explained in the 'Discussion' section.

The specimens nested in the subclade of *X. lanatus* s. str. (Figs. 2 and 3) are morphologically similar to *X. lanatus* holotype and epitype, except H 7200692. The latter has a poorly developed, discontinuous subiculum, fragile aculei, and it lacks a well-developed sterile margin (Fig. 5b). According to these macroscopic features, it is close to the holotype of *X. pseudolanatus* (see Riebesehl et al. 2019). A similar discrepancy was observed for H 7200690, nested within the *X. pseudolanatus* subclade. This specimen has a well-developed subiculum and sterile margin, like in *X. lanatus* s. str. (Fig. 5c). Thus, we conclude that subiculum and margin morphology in *X. lanatus* and *X. pseudolanatus* may be affected by growth conditions. However, we have found a difference in hymenophoral aculei size: within an individual basidioma the aculei are in average smaller in *X. pseudolanatus* (see the key below). Moreover, aculei in *X. pseudolanatus* are less bristly, with more compactly arranged hyphoid cystidia, than in *X. lanatus*.

Thorough microscopy for tens of sections of specimens belonging to the different subclades of *X. lanatus* s. l. showed that spore morphology (Fig. 6) and cystidial morphology can be used to distinguish species, which together with phylogenetic evidence allowed us to describe two more species in this complex: *X. afromontanus* (Fig. 5d) and *X. mantiqueirensis* (Fig. 5e).

We have found two specimens from Borneo and one from Java, which fit in most morphological features to the protologue and to the holotype of *X. echinatus* (Fig. 5f). The specimen from Java (H 7200350) differs from the original description of *X. echinatus* by slightly smaller spores, (4.5−)5−5.8 × (3.3−)3.5−4(−5) µm. The specimens from Sunda Archipelago also have fewer echinulate crystals on projecting hyphae, than in the holotype (Fig. 7).

After studying the holotype of *Pteridomyces sphaericosporus* Boidin, Lanquetin & Gilles (LY 7377), we found it identical in cystidial, hyphal and spore morphology with *Xylodon hyphodontinus*, depicted in Riebesehl et al. (2019, Fig. 6), and so re-affirm that *P. sphaericosporus* is a synonym of *X. hyphodontinus*.

In the present study we have distinguished two more species, collected in South America, with globose to broadly ellipsoid spores and an odontioid hymenophore. The specimens BLS M-5234, BLS M-5235, collected in Ecuador, and SP467086, collected in Brazil, demonstrated such high degree of morphological similarity, that we classify them in one species, *X. neotropicus*, which is supported by the phylogenetic analyses. The species, found in Ecuador and named *X. gloeocystidiifer*, is represented by two specimens, BLS M-5232 and EYu 190720-11 (CFMR), which are identical in most macroscopic and microscopic features, but do not fit to any earlier described species of *Xylodon*. The protologues of *X. neotropicus* and *X. gloeocystidiifer* are given in the 'Taxonomy' section.

We carried out SEM study of crystalline deposits on projecting hyphae (hyphoid cystidia) of *Xylodon* species (Fig. 7). With this, we aimed to find additional features to distinguish species in *X. lanatus* s. l. The specimens of *X. lanatus* (CFMR HHB-8925, CFMR FP-101864-A, CFMR FP-102919, H 7200692), *X. pseudolanatus* (CFMR FP-150922, H 7200690), *X. afromontanus* (O-F-904012, H 7006854), *X. mantiqueirensis* (H 7075551) and *X. echinatus* (TNM F24751, H 7200350) were examined. Plate-like crystals, 2−4 µm in diameter, with serrate margins, aggregated in rose-shaped structures, were observed in all listed specimens as the predominating morphological type of deposits. Morphological differences for these crystals were small: they were more aggregated in stacks and not so rose-shaped in *X. afromontanus* (Fig. 7c), and on average smaller (about 2 µm diam.) in *X. mantiqueirensis* (Fig. 7d). Moreover, crystals without serrate margins were observed in *X. echinatus* (Fig. 7f) and *X. afromontanus*. Bipyramidal crystals were rare on hyphoid cystidia (Fig. 7b, c, f), but were more common on subicular hyphae.

Taxonomy

Xylodon lanatus (Burds & Nakasone) Hjorstam & Ryvarden

Basionym: *Hyphodontia lanata* Burds & Nakasone, Mycologia 73: 461 (1981).

Epitype (designated here, MycoBank Typification No.: 10013103): USA. Mississippi, Harrison County, De Soto National Forest, Harrison Experimental Forest, 30.6305° N, 89.0456° W, on dead hardwood, leg. K.K. Nakasone, 5 Nov 1981 (CFMR FP-101864-A; Figs. 5a, 6a).

Basidiomata effused, fragile membranaceous. Subiculum continuous, 70−170 µm thick, of open, woolly texture, pale brownish yellow. Hymenial surface

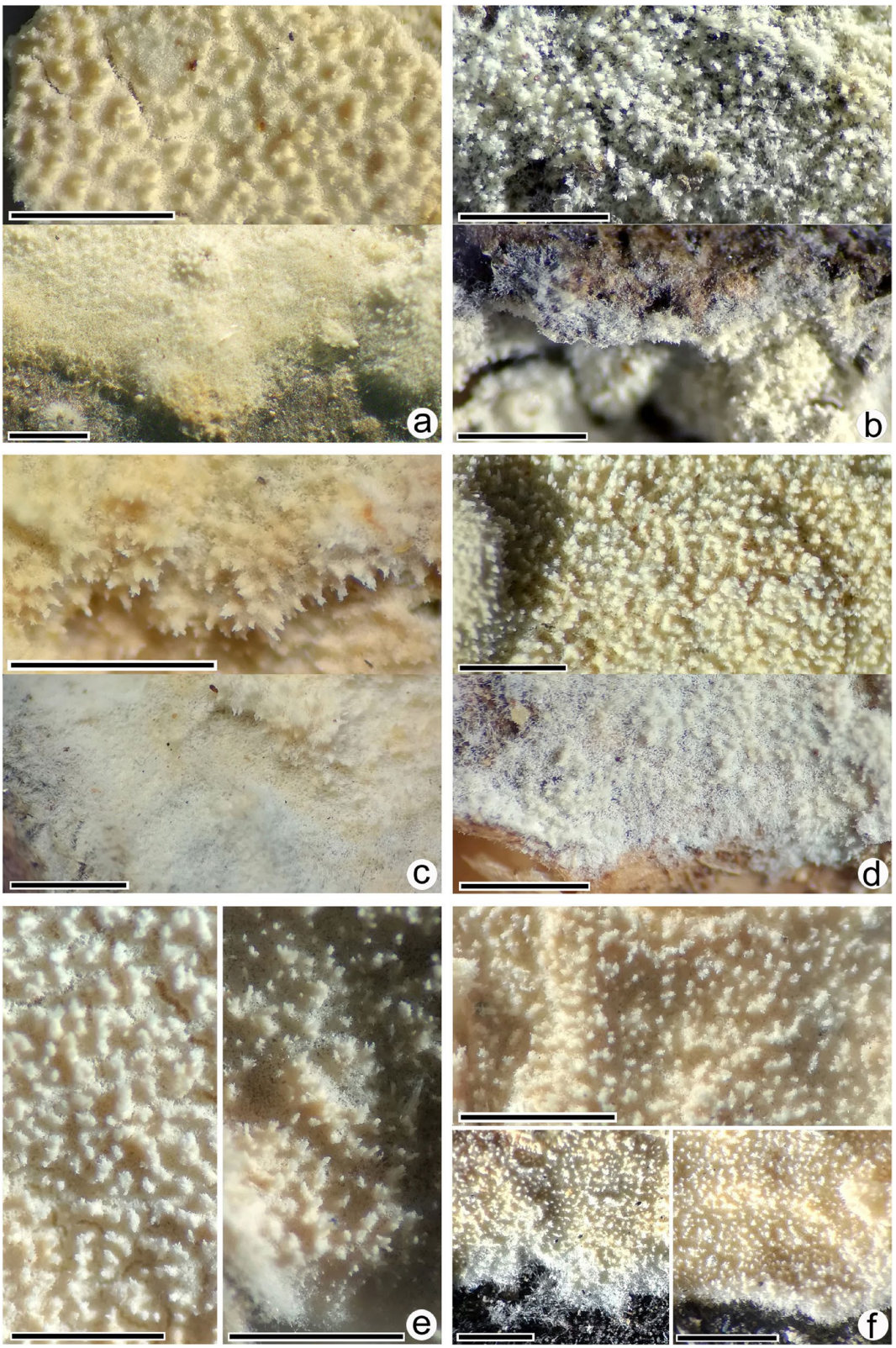

Fig. 5 Macromorphology of *Xylodon lanatus* s. l. **a** *X. lanatus*, epitype (CFMR FP-101864-A); **b** *X. lanatus* (H 7200692); **c** *X. pseudolanatus* (H 7200690); **d** *X. afromontanus*, holotype (O-F-904012); **e** *X. mantiqueirensis*, isotype (H 7075551); **f** *X. echinatus* (H 7200350). In **a**–**d**, **f** the upper images show central part of basidioma, lower images show the margin of basidioma. Scale bars = 1 mm

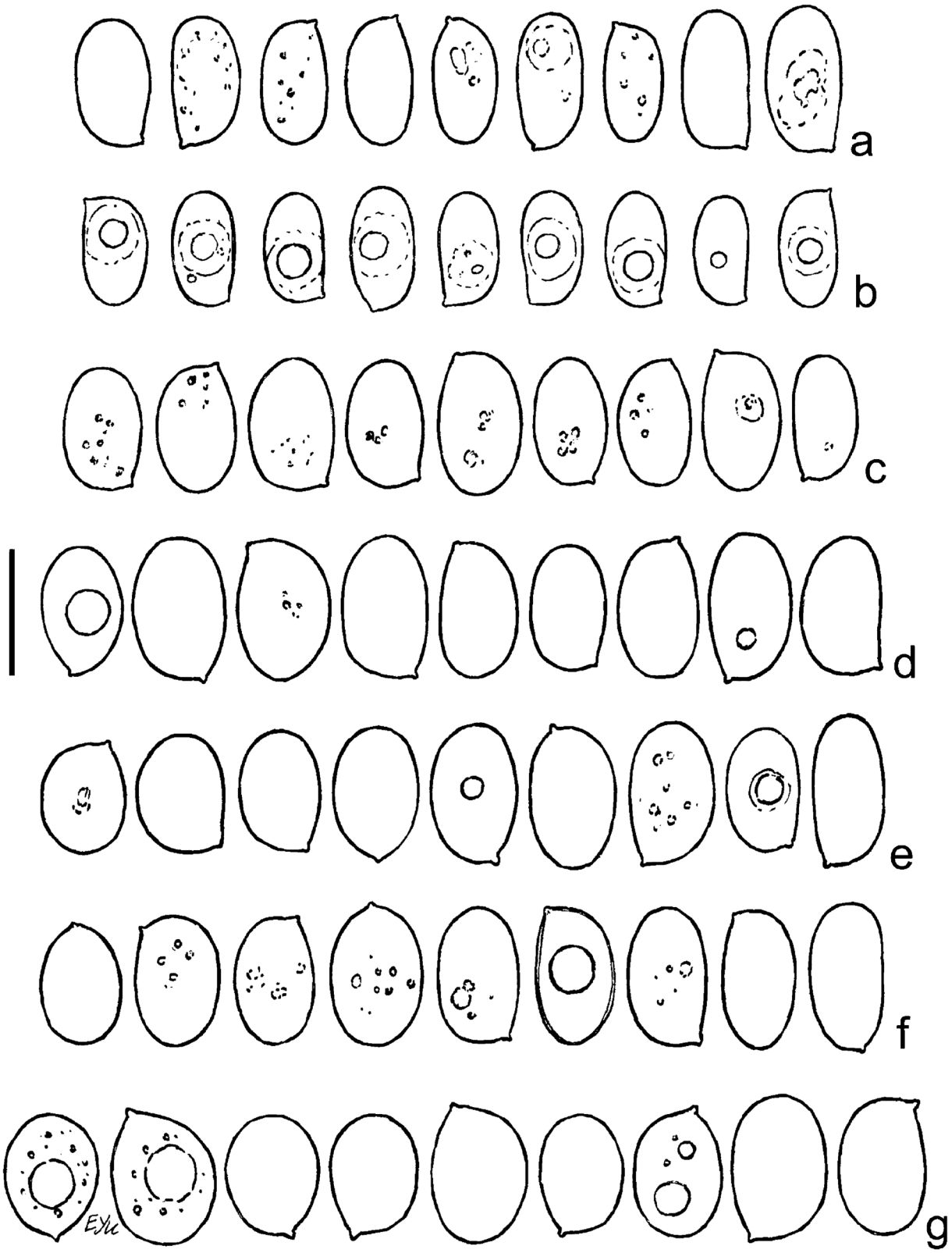

Fig. 6 Basidiospores in the *Xylodon lanatus* species complex. **a** *X. lanatus*, epitype (CFMR FP-101864-A); **b** *X. lanatus* (KAS-Ec720); **c** *X. pseudolanatus* (CFMR HHB-4305); **d** *X. pseudolanatus* (H 7200690); **e** *X. afromontanus*, holotype (O-F-904012); **f** *X. mantiqueirensis*, isotype (H 7075551); **g** *X. echinatus* (H 7200350). Scale bar = 5 µm

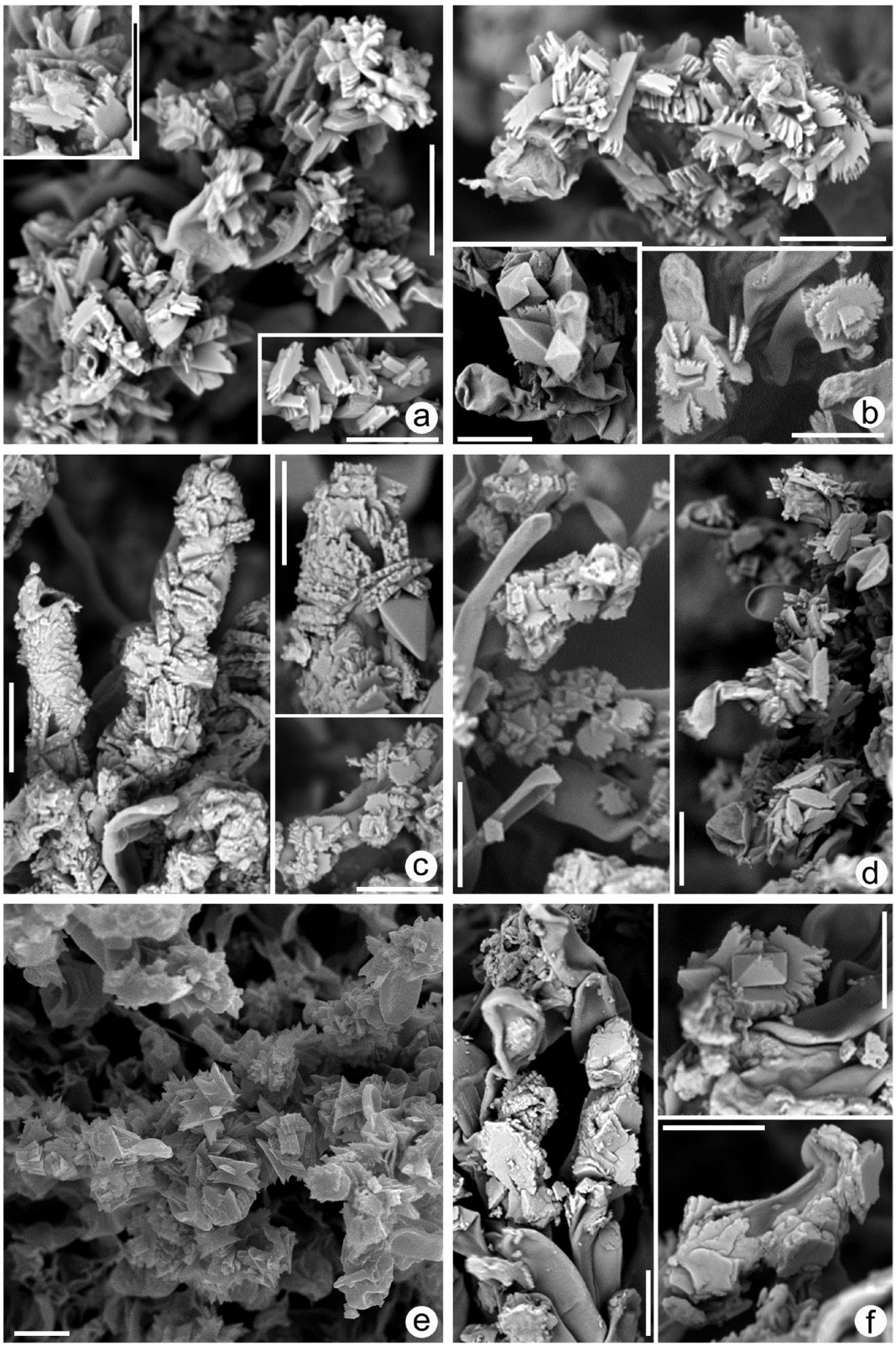

Fig. 7 SEM images of crystalline deposits on projecting hyphae in hymenophoral aculei of *Xylodon lanatus* s. l. **a** *X. lanatus*, holotype (CFMR HHB-8925); **b** *X. pseudolanatus*, holotype (CFMR FP-150922); **c** *X. afromontanus*, holotype (O-F-904012); **d** *X. mantiqueirensis*, isotype (H 7075551). **e** *X. echinatus*, holotype (TNM F24751); **f** *X. echinatus* (H 7200350). Scale bars = 5 µm

odontioid, cream-coloured; aculei irregularly conical or irregularly cylindrical, 4−6/mm, (40−)65−200 µm high, (30−)60−140(−170) µm diam. at base, (25−)30−95 µm diam. in the middle part. The part between aculei continuous, 60−200 µm thick. Margin woolly, 1−1.5 mm wide, of the same colour as hymenial surface. Hyphal system monomitic, hyphae colourless, clamped at all primary septa. Subicular hyphae sparingly branched, 2−4 µm wide, with some inflations up to 5−6 µm wide, thin- to thick-walled (wall up to 1 µm thick), smooth or with isodiametric crystals, 1.5−4(−7) µm across, scattered between hyphae. Subhymenial hyphae moderately to richly branched, (1.3−)1.7−3 µm wide, moderately thin-walled under basidia, slightly thick-walled in lower subhymenium, smooth to fairly richly encrusted by crystals reaching 5−12 µm across. Projecting hyphae at aculeal apices (hyphoid cystidia) mostly collected in clusters, almost straight to flexuous, 20−50 × 2.3−4 µm, thin- to thick-walled (wall up to 1.3 µm thick), even or with some constrictions, loosely encrusted, predominantly near apex, sometimes smooth. Immersed capitate or clavate-capitate cystidia (vesicular structures) 10−40 × (4−)5−8.5(−9) µm, often with 1−4 adventitious septa, thin- to thick-walled (wall in swollen part up to 1.5 µm thick). Capitate cystidia in hymenium rare, 13−30 × 3−5 µm, thin-walled. Basidioles subcylindrical to clavate, (8−)12−20(−27) × 3.2−4.5(−5.5) µm, thin-walled, smooth or poorly encrusted. Basidia narrowly utriform, thin-walled, smooth, 20−25 × 3.5−4 µm, with four sterigmata 2−2.5 × 0.5 µm. Basidiospores narrowly ellipsoid to oblong, (4.5−)5.3−5.7(−6) × (2.5−)2.7−3.5 µm (in epitype $L = 5.3$ µm, $W = 2.9$ µm), $Q = 1.7−2.2$, barely thick-walled, Mz−, acyanophilous, with very short or unclear apiculus.

Remark: In holotype (CFMR HHB-8925) basidiospores are 4.5−5.5 × 2.5−3(−3.3) µm, with $L = 4.95$ µm and $W = 2.8$ µm.

Additional specimens examined: USA. Mississippi, Harrison County, De Soto National Forest, 'Hammock Road H 4-Harrison Experimental Forest', on dead wood of *Liriodendron tulipifera*, coll. H.H. Burdsall, Jr., 1 Apr 1976 (CFMR HHB-8925, holotype); North Carolina, Brunswick County, Green Swamp Preserve, swamp forest with canopy of *Pinus* with admixture of *Acer rubra*, on fallen branch of angiosperm, leg. O. Miettinen, 16 Nov 2013, OM 17683 (H 7200691); Florida, Alachua County, Gainesville, Sweetwater Preserve, middle-aged mixed forest, on dead wood of angiosperm, leg. O. Miettinen, 22 Nov 2013, OM 17835.3 (H 7200692); Puerto Rico, Maricao Commonwealth Forest, Near Maricao Recreation Area, 18.1723° N, 66.9861° W, on dead wood, leg. K.K. Nakasone, 25 Jun 1996 (CFMR FP-102919-Sp). Ecuador. Zamora Chinchipe Province, the vicinity of Estación Científica San Francisco, Permanent sample plot No. 5, about 1850 m a.s.l., on log with no contact to ground, leg. E. Langer, 8 Mar 2002 (KAS-Ec720).

***Xylodon afromontanus* Yurchenko & Viner, sp. nov.**

Figs. 5d, 6e, 7c.

MycoBank No.: MB848555.

Etymology: the specific epithet stresses the origin of the type material from mountains of Africa.

Holotype: Rwanda. Western Province, Nyungwe Forest National Park, trail from Pindura to Mount Bigugu, 2750 m a.s.l., on decayed corticated branch, leg. J. Rammeloo, 29 Jul 1974, No. 4115 (O-F-904012; isotype H 7006811).

Basidiomata effused, 2–4 and more cm in extent, fragile membranaceous, between aculei loose, 60–140 µm thick. Hymenial surface odontioid, pale cream to cream-coloured; aculei irregularly conical, usually fimbriate, 50–85 µm high, 40–85 µm diam., 5−7/mm. Margin thinning out or mould-like, 0.1–0.5 mm wide, concolourous or paler than fertile part of basidioma. Hyphal system monomitic, hyphae clamped at all septa, moderately branched, colourless. Subicular hyphae 2.5–3.5 µm wide, with scattered inflations up to 9 µm wide, with thickened or thick (up to about 1 µm) walls, smooth or scarcely incrusted. Subhymenial hyphae (2–)2.5–3.2 µm wide, walls thin, sometimes thick near subiculum, smooth or encrusted by crystals 2–3 µm across. Projecting hyphae (hyphoid cystidia) almost straight to flexuous, 30–50(–80) × (2–)2.5–3.5 µm, smooth to encrusted, especially in upper part, thin- to thick-walled (wall up to 1 µm thick), without or with occasional constrictions. Cystidia rare, capitate and clavate, (13–)25–35 × 5–8 µm, thin-walled in apical part, lacked adventitious septa; also present cystidia little differentiated from hyphal ends (subcapitate and subclavate). Basidioles clavate, subcylindrical, occasionally subcapitate, (7–)15–23 × 4–5 µm, smooth or slightly encrusted. Basidia narrowly utriform, 20−25(–30) × 4−4.5(–5) µm, thin-walled, smooth or slightly encrusted, with four sterigmata 2.5–3.5 × 1 µm. Basidiospores broadly ellipsoid ($Q = 1.3$) to narrowly ellipsoid ($Q = 1.8−2.2$), with a prevalence of ellipsoid ones ($Q = 1.5−1.6$), (4.3−)5−6(−6.5) × 3−4 µm, thin-walled, Mz–, acyanophilous; apiculus very short or unclear.

Distribution and ecology: The species occurs in Eastern Africa, in Afromontane rainforests at the elevations about 1800−2800 m a.s.l. and grows saprobically on dead wood.

Remarks: A notable feature of this species is the presence of variable, broadly ellipsoid to narrowly ellipsoid basidiospores, within the same basidioma. In the holotype spores are (4.3−)4.7−6 × 3−4 µm ($L = 5.2$ µm, $W = 3.5$ µm), in the paratype they are 5−6(−6.5) × 3−4 µm ($L = 5.6$ µm, $W = 3.5$ µm). The distinctions of this species from other members of *X. lanatus* complex are described in the key below.

Additional specimen examined: Malawi. Southern Region, Mulanje distr., Mulanje Massif, Lichenya Plateau, 1800−2000 m a.s.l., on dead decorticated wood, leg. L. Ryvarden, 9−10 Mar 1973, No. 11416 (O-F-904167; dupl. H 7006854).

Xylodon mantiqueirensis **Yurchenko, Motato-Vásq. & Viner, sp. nov.**

Figs. 5e, 6f, 7d.

MycoBank No.: MB848556.

Etymology: *mantiqueirensis* = occurring in the Mantiqueira Mountains (Serra da Mantiqueira), a chain northeast of São Paulo.

Holotype: Brazil. São Paulo State, the vicinity of Campos do Jordão, Parque Estadual Campos do Jordão, Celestina trail, *Araucaria* forest, on dead decaying branch, leg. V. Motato-Vásquez, A.M. Gugliotta, J. Cabra-García, 14 Oct 2015, MV529 (SP467059; isotype H 7075551).

Basidiomata effused, 10–15 and more cm in extent, membranaceous, between aculei slightly cracking, 180–250 µm thick. Hymenial surface odontioid, cream-coloured; aculei conical or subcylindrical, often fimbriate apically, 60–180 µm high, 30–75 µm in diam., 4−7/mm. Margin fimbriate to woolly, 0.5–1 mm wide, concolourous or paler than the fertile part of basidioma. Hyphal system monomitic, hyphae clamped at all septa, colourless. Subiculum loose, woolly; subucular hyphae moderately branched, 2.7–4(–4.5) µm wide, with thickened or thick (up to 1.3 µm) walls, smooth. Subhymenial hyphae moderately to richly branched, 2–3 µm wide, walls thin or slightly thickened near subiculum, smooth or scarcely encrusted. Projecting hyphae (hyphoid cystidia) almost straight to flexuous, (25–)30–50(–80) × 2.5–3.5(–4) µm, smooth to encrusted, especially in upper part, thin- to thick-walled (wall up to 1 µm thick), with scattered constrictions. Cystidia capitate, 20–35 × (5–)5.5–9 µm, with 0–2 adventitious septa, in capitate part thin- or slightly thick-walled. Basidioles clavate, subcapitate, capitate, rarely subcylindrical, (10–)13–25 × 3.5–6.5 µm, smooth. Basidia narrowly utriform, 17–31 × 4–4.5 µm, thin-walled, smooth. Basidiospores from broadly ellipsoid (Q = 1.4) to predominantly narrowly ellipsoid (Q = 1.6–1.7), 5−6 × (2.5−)3−3.5 µm (in holotype L = 5.3 µm, W = 3.1 µm), Mz–, acyanophilous; apiculus short or unclear.

Distribution and ecology: The species is known so far from tropical montane forests in the southeastern Brazil; it grows saprobically on dead wood.

Remarks: A distinctive feature of this species is common subcapitate and capitate thin-walled elements in hymenium, which can be treated as basidioles or small cystidia. Basidiospores in this species are of variable shape within the same basidioma. In contrast to *X. afromontanus*, ellipsoid spores (Q = 1.4–1.5) in *X. mantiqueirensis* are few. Other distinctions of *X. mantiqueirensis* from the members of *X. lanatus* complex are described in the key below.

Additional specimen examined: Brazil. São Paulo State, the same address as holotype, *Araucaria* forest, on decaying wood, leg. V. Motato-Vásquez, A.M. Gugliotta, J. Cabra-García, 14 Oct 2015, MV509 (SP498889).

Key to the species of *Xylodon lanatus* complex

1. Ellipsoid to broadly ellipsoid basidiospores (Q = 1.3–1.5) present, from rare to common ….....2
- Spores with Q = 1.3–1.5 absent or occasional; most spores ellipsoid to narrowly ellipsoid and short cylindrical (Q = 1.6–2.1) 4
2. Capitate cystidia with thick wall and/or adventitious septa absent; pronounced constrictions on projecting hyphae (hyphoid cystidia) absent or occasional …..... 3
- Some capitate cystidia with thick wall and/or adventitious septa; pronounced constrictions present on some projecting hyphae (hyphoid cystidia); the species found in the eastern part of South America …..... *X. mantiqueirensis*
3. Basidioma between aculei often more than 150 µm thick, up to 350 µm thick; sterile margin woolly, continuous; species, occurring in Southeast Asia …..... *X. echinatus*
- Basidioma between aculei usually less than 140 µm thick; sterile margin thinning out, discontinuous; species, occurring in eastern Africa ..... *X. afromontanus*
4. Hymenophoral aculei 0.13–0.35 mm long, 4 per mm; species, occurring in New Zealand …..... *X. vesiculosus*
- Hymenophoral aculei 0.05–0.125 mm long, 4–9 per mm; species from North America, South America and Southeast Asia …..... 5
5. Projecting hyphae (hyphoid cystidia) mostly flexuous and with distinct constrictions, with thin or thickened walls; Asian species …..... *X. kunmingensis*
- Projecting hyphae (hyphoid cystidia) mostly straight or somewhat wavy and without constrictions; if constricted, then with thickened or thick walls; American species … 6
6. Well-developed hymenophoral aculei 60–140 µm in diameter at base and 30–95 µm in diameter in the middle part; all spores ellipsoid to narrowly ellipsoid, Q = 1.6–2.1 ….. ..... *X. lanatus* s. str.
- Well-developed hymenophoral aculei 40–90 µm in diameter at base and 30–60 µm in diameter in the middle part; some spores almost broadly ellipsoid (Q = 1.4–1.5) .... *X. pseudolanatus*

Xylodon neotropicus **Yurchenko, Motato-Vásq. & Viner, sp. nov.**

Figs. 8, 9.

MycoBank No.: MB848557.

Etymology: *neotropicus* (Lat.) = occurring in the Neotropics.

Holotype: Brazil. Rio de Janeiro State, Serra da Mantiqueira Mts., Parque National do Itatiaia, Três Picos trail, 22.3483°S, 44.6208°W, Atlantic rainforest, on dead decaying corticated branch, leg. V. Motato-Vásquez, A.M. Gugliotta, 27 Nov 2015, MV580 (SP467086; isotype H 7075552).

Basidiomata effused, membranaceous, fairly tough in old state, up to 5 and more cm long, 0.1–0.2 mm thick between aculei. Margin thinning out. Hymenial surface odontioid to short hydnoid and almost irpicoid, from yellowish with ochraceous tinge to ochraceous. Aculei conical or flattened, subirpicoid, about 2.5/mm, partly confluent at bases, up to 1 mm high, 0.2–0.8 mm wide. Hyphal system monomitic, hyphae clamped at all primary septa, colourless or yellowish in mass. Subicular and tramal hyphae (1.7–)2.5–3.5(–4.5) µm wide, thin- to mostly thick-walled (walls up to 1 µm thick), smooth or with scarce coarse crystals 8–12 µm across. Subhymenial hyphae richly branched, 1.2–3.5(–4.3) µm wide, with short and somewhat swollen segments, thin- to slightly thick-walled towards subiculum, smooth or with minutely rough surface. Hymenial surface with numerous projecting peg-like aggregates of loosely encrusted hyphae, 35–70 µm long, 13−22 µm wide, giving to the aculei asperulate or setose appearance under a lens; individual hyphal ends in pegs thin-walled, (1.8−)2.3–3.2 µm wide, 3.5–4.5 µm wide with incrustation, apically cylindrical or slightly narrowing. Cystidial elements (cystidioles) in hymenium thin-walled, of three types: (1) fusoid rare, smooth, 13–21 × 3.5–5.5 µm; (2) cylindrical or subcylindrical rare, 12–21 × 3.5–4.5

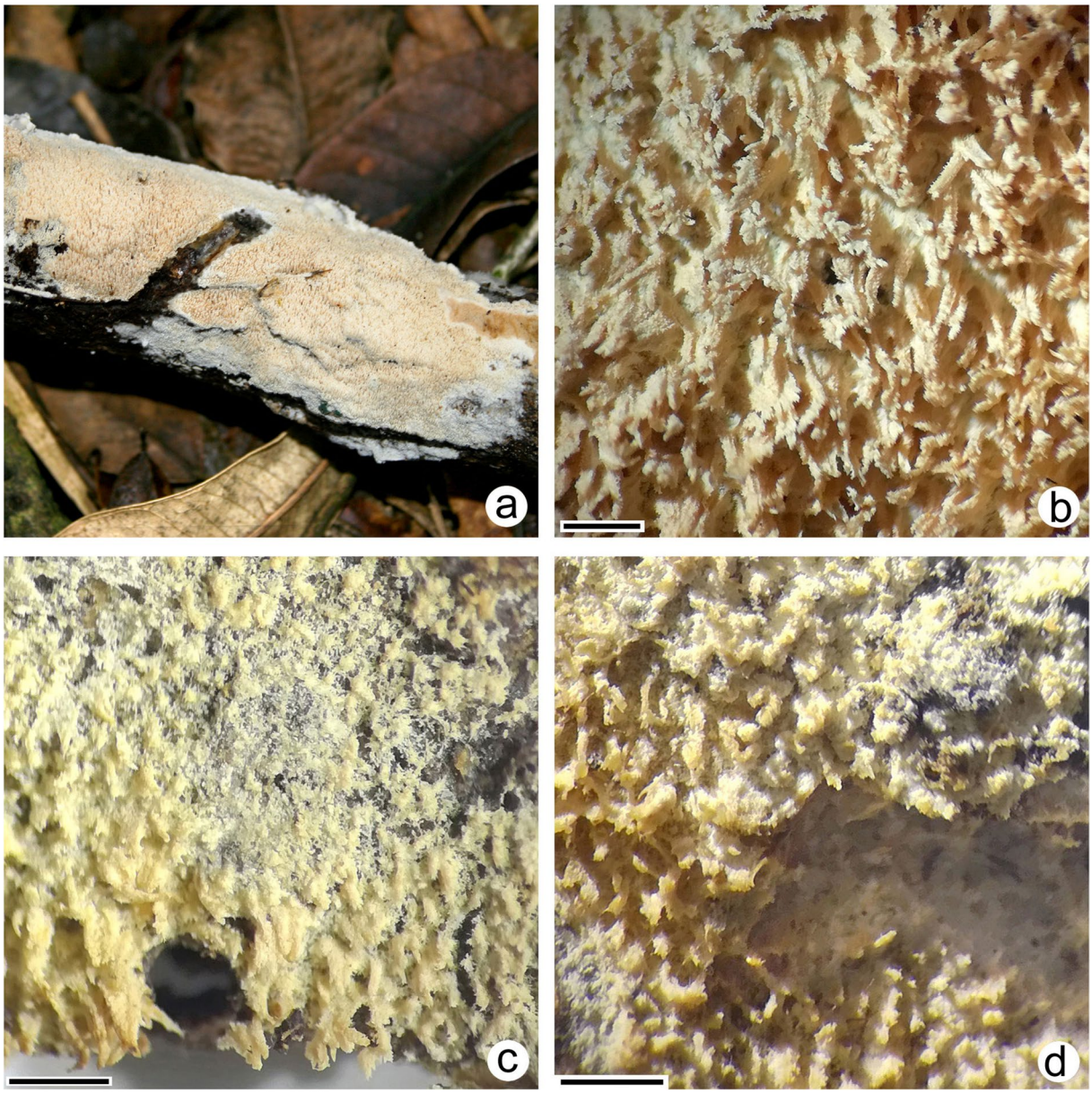

Fig. 8 Macromorphology of *Xylodon neotropicus*. **a** A basidioma in type locality of the species; **b** isotype (H 7075552), basidioma in central part; **c** isotype, periphery of basidioma; **d** paratype (BLS M-5234). Scale bars = 1 mm

µm, often widened at base, smooth or scarcely encrusted; (3) capitate rare, 10–16.5 × 3.5–4.5 µm, smooth. Basidioles from ovoid to subcylindrical, 5.5−15(–18) × 3−5 µm, smooth. Basidia subcylindrical-subutriform, 11–12 × 3.5–4.3 µm; sterigmata four, about 2.5 × 0.5 µm. Basidiospores globose to subglobose, 3.5–4(–4.5) × 3.3–3.7(–4) µm (in holotype L = 3.85 µm, W = 3.55 µm), thin- to slightly thick-walled, colourless, Mz–, acyanophilous; apiculus short and blunt, distinct, sometimes unclear.

Distribution and ecology: The species is known from northeastern Ecuador and southeastern Brazil, and grows on dead branches. The natural range of this species supposedly covers the part of South America where tropical humid forests occur.

Remarks: The species is morphologically most close to *X. hyphodontinus* due to clusters of projecting encrusted hyphae, fusoid cystidia (cystidioles), inflated hyphae in subhymenium, and globose basidiospores. However, *X. neotropicus* has much larger hymenophoral aculei, and ochraceous colour or hymenial surface, which was never noted in *X. hyphodontinus*. BLS M-5233 is a form of *X. neotropicus*, which differs from three other specimens of this species by the presence of scattered, shortly clavate and pyriform basidioles 6.5–9 × 4.5–5.5 µm, covered by crystalline encrustations.

Additional specimens examined: Ecuador. Orellana Province, near Flor de Oriente village, 0.5042°S, 76.9819°W, 295 m a.s.l., equatorial rainforest in hilly area, on fallen branch, leg. E. Yurchenko, 21 Jul 2019, EYu 190721-12a (BLS M-5235), EYu 190721-12b (BLS M-5234); between Puerto Francisco de Orellana and El Dorado, right bank of the Napo river, 0.4861°S, 76.9500°W, 260 m a.s.l., Amazonian rainforest, on dead hanging decorticated branch, leg. E. Yurchenko, 20 Jul 2019, EYu 190720-12a (BLS M-5233).

Xylodon gloeocystidiifer **Yurchenko & Riebesehl, sp. nov.**
Figs. 10, 11.

MycoBank No.: MB848558.

Etymology: *gloeocystidiifer* (Lat.) = bearing gloeocystidia.

Holotype: Ecuador. Orellana Province, near Flor de Oriente village, 0.5042°S, 76.9819°W, 295 m a.s.l., equatorial rainforest in hilly area, on large fallen decaying leaf, leg. E. Yurchenko, 21 Jul 2019, EYu 190721-61 (BLS M-5232).

Basidioma effused, 0.5–1.5 cm in extent, membranaceous, minutely odontioid; the part between aculei loose, discontinuous, 50−120 µm thick, white. Aculei 5−6/mm, conical, simple or branched/aggregated, fimbriate, often apically attenuated, 70−180 µm long, 70−140 µm diam., from white to yellowish and pale ochraceous. Margin more or less thinning out. Hyphal system monomitic, hyphae clamped at all septa, colourless, but tramal hyphae becoming yellowish in mass with age. Subicular hyphae sparsely branched, colourless, thin- to thick-walled (wall up to 0.8 µm thick), 2.3−3.5 µm wide; coarse crystals up to 10−15 µm across scattered between hyphae. Tramal hyphae sparsely branched, more or less parallel (vertically arranged), 2−3 µm wide, thin- to slightly thick-walled, smooth or slightly encrusted, colourless or yellowish in mass, protruding in aculeal apices as bundles of hyphal ends; hyphae in these bundles 2.5−4.3 µm wide, usually agglutinated, smooth, apically rounded, rarely subcapitate, capitulate (capitulus about 2 µm wide) or collapsed and then tapering. Subhymenial hyphae moderately or richly branched, 1.8−3 µm wide, thin-walled, smooth or scarcely encrusted. Cystidia of two types: (1) capitate numerous, colourless to yellowish, 12−20 × 3−4 µm, with fragile apex 4−5 µm wide; apical swelling slightly refractive, in older basidiomata supplied by a cap of resinous matter 9−12 µm wide; caps preserved in water and CB, but easily dissolving in KOH; (2) gloeocystidia subcylindrical or fusoid, 10−30(−35) × (4−)5−6(−6.5) µm, slightly refractive and pale yellowish in KOH, with the contents becoming coloured in Mz and CB. Basidioles ovoid, short clavate, subcylindrical, 6.5–13 × (3.2−)3.5–4.3 µm, colourless to yellowish. Basidia subcylindrical or subutriform, 10−18.5 × (3−)3.3−4.3 µm; sterigmata four, 1.7–3.5 × 0.3–0.5 µm. Basidiospores globose to broadly ellipsoid, mostly subglobose, (3.2−)3.5−4(−4.5) × 2.8−3.5(−3.7) µm (in holotype L = 3.9 µm, W = 3.3 µm), slightly or unclearly thick-walled, colourless, Mz–, acyanophilous; apiculus minute, narrow or little pronounced.

Distribution and ecology: The known localities are in northeastern part of Ecuador, in zone of Amazonian rainforest, the Napo river basin. The fungus grows saprobically on wooden and non-wooden remains, like decayed leaves.

Remarks: In hymenium of this fungus there are also elements, intermediate in morphology between basidioles and gloeocystidia, basidioles and capitate cystidia, gloeocystidia and capitate cystidia. Thickened spore wall is more clearly visible in Mz.

There are several species of *Xylodon*, possessing, like *X. gloeocystidiifer*, cylindrical/subcylindrical cystidia and capitate cystidia with resinous caps: *X. brevisetus, X. crassisporus*, *X. spathulatus*, *X. subclavatus*. The main differences of these from *X. gloeocystidiifer* are: much loose texture of aculei and ellipsoid spores in *X. brevisetus*, longer leptocystidia and ellipsoid spores in *X. crassisporus*, loose arrangement of hyphae at apices of aculei and cystidia with narrowed tips in *X. spathulatus*, moniliform cystidia in *X. subclavatus*. Besides, the new species has similarities with *X. follis*, but the latter has projecting hyphae with crystalline incrustation, vesicular basidioles and much larger spores.

Additional specimen examined: Ecuador. Orellana Province, between Puerto Francisco de Orellana town and El Dorado village, right bank of the Napo river, 0.4861°S, 76.9500°W, 260 m a.s.l., equatorial rainforest, on fallen corticated piece of wood, leg. E. Yurchenko, 20 Jul 2019, EYu 190720-11 (CFMR).

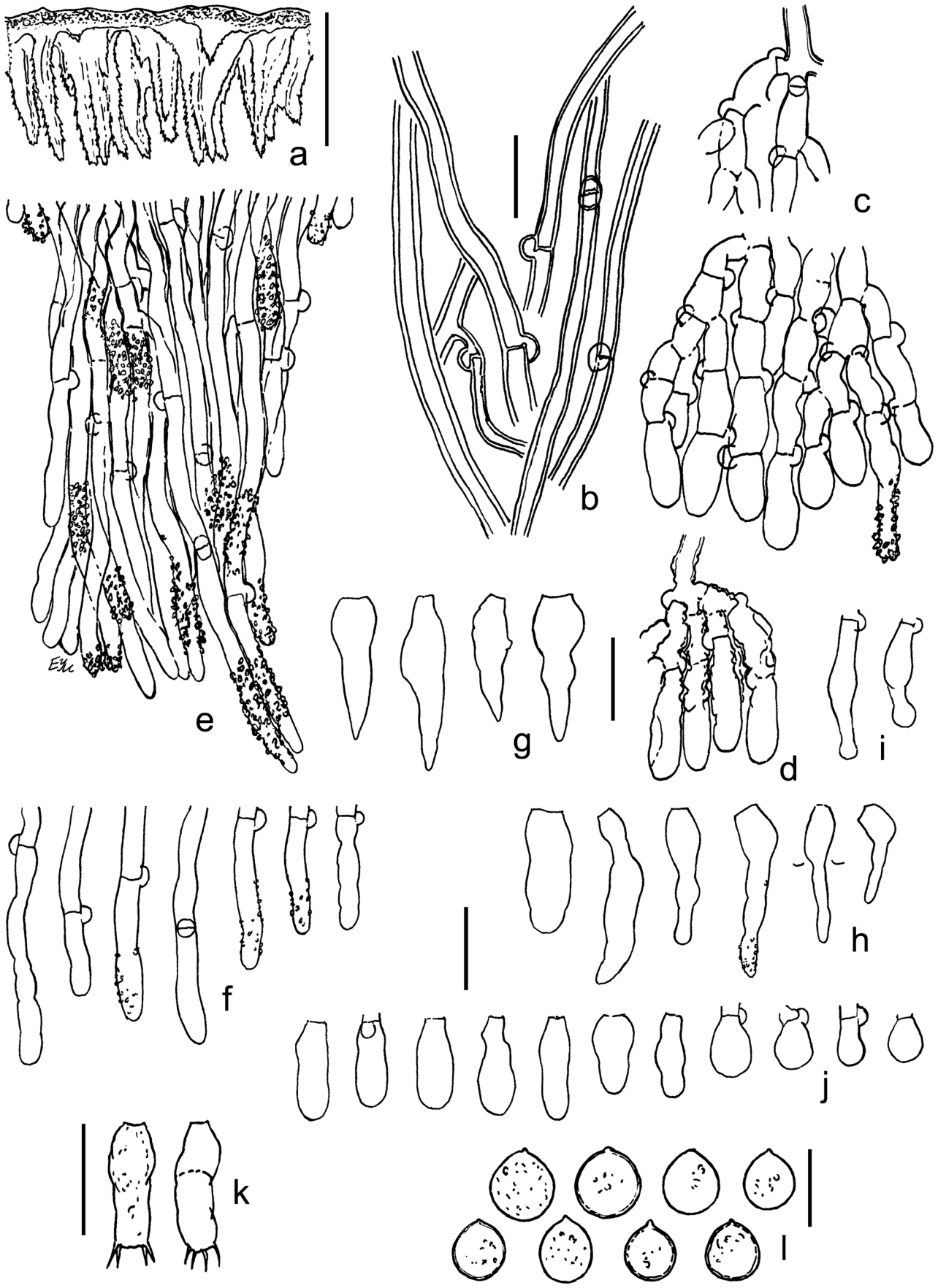
a
b
c
d
e
f
g
h
i
j
k
l

◂**Fig. 9** Micromorphology of *Xylodon neotropicus* (isotype, H 7075552). **a** Vertical section through basidioma; **b** hyphae of aculeal trama; **c** portion of hymenium and subhymenium; **d** subbasidial hyphae with rough surface; **e** peg-like aggregate of hyphae; **f** individual hyphae projecting from the hymenium; **g** fusoid cystidia; **h** cylindrical and subcylindrical cystidia; **i** capitate cystidia; **j** basidioles; **k** basidia; **l** basidiospores. **b**, **c**, **e**–**l** preparations in KOH; **d** preparation in Mz. Scale bars = 1 mm for **a**, 10 µm for **b**–**k**, 5 µm for **l**

Xylodon yunnanensis* and *Hyphodontia yunnanensis

The BLAST search and the reconstruction of phylogeny (Fig. 1) demonstrated that the taxa called *Xylodon yunnanensis* (with holotype LWZ 20180920-12a (HMAS)) and *Hyphodontia yunnanensis* (with holotype SWFC 6804) belong to the same species. This is also apparent after comparison of the protologues of *X. yunnanensis* (Wang et al. 2021) and *H. yunnanensis* (Boonmee et al. 2021): the cystidial elements, hyphae and spores in these fungi were described as slightly different at best. Both holotypes originate from the same geographic area (Yunnan Province, Chuxiong, Zixi (Zixishan) Forest Park), and were collected in the same year (2018). Because of the priority of publishing date, 12 June 2021 for *X. yunnanesis* against 7 December 2021 for *H. yunnanensis*, and taking into account the incorrect placement of the material in *Hyphodontia*, we propose

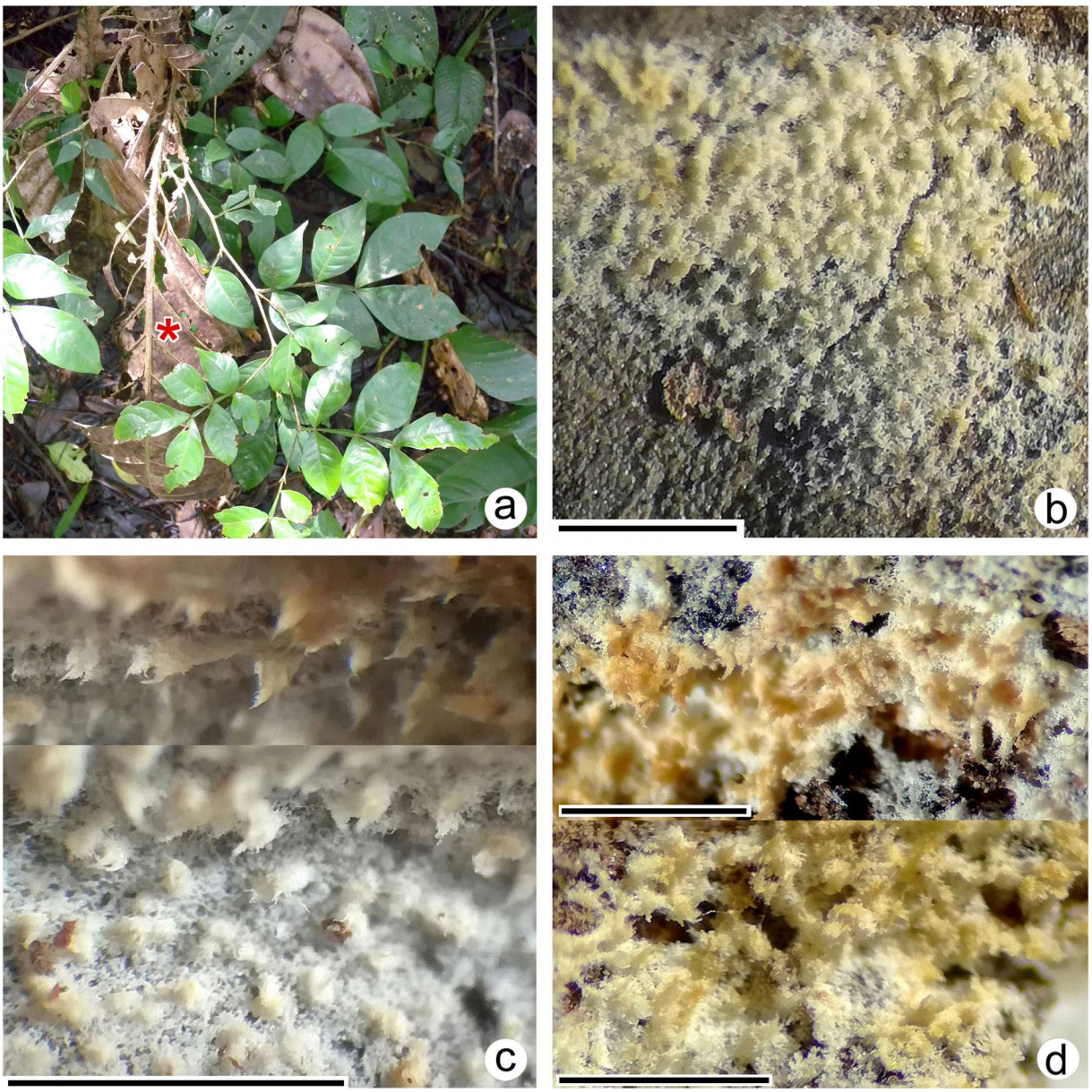

Fig. 10 Habitat and macromorphology of *Xylodon gloeocystidiifer*. **a** Substratum of the holotype (BLS M-5232) in situ (marked *); **b**, **c** holotype; **d** paratype (EYu 190720-11 (CFMR)). Scale bars = 1 mm

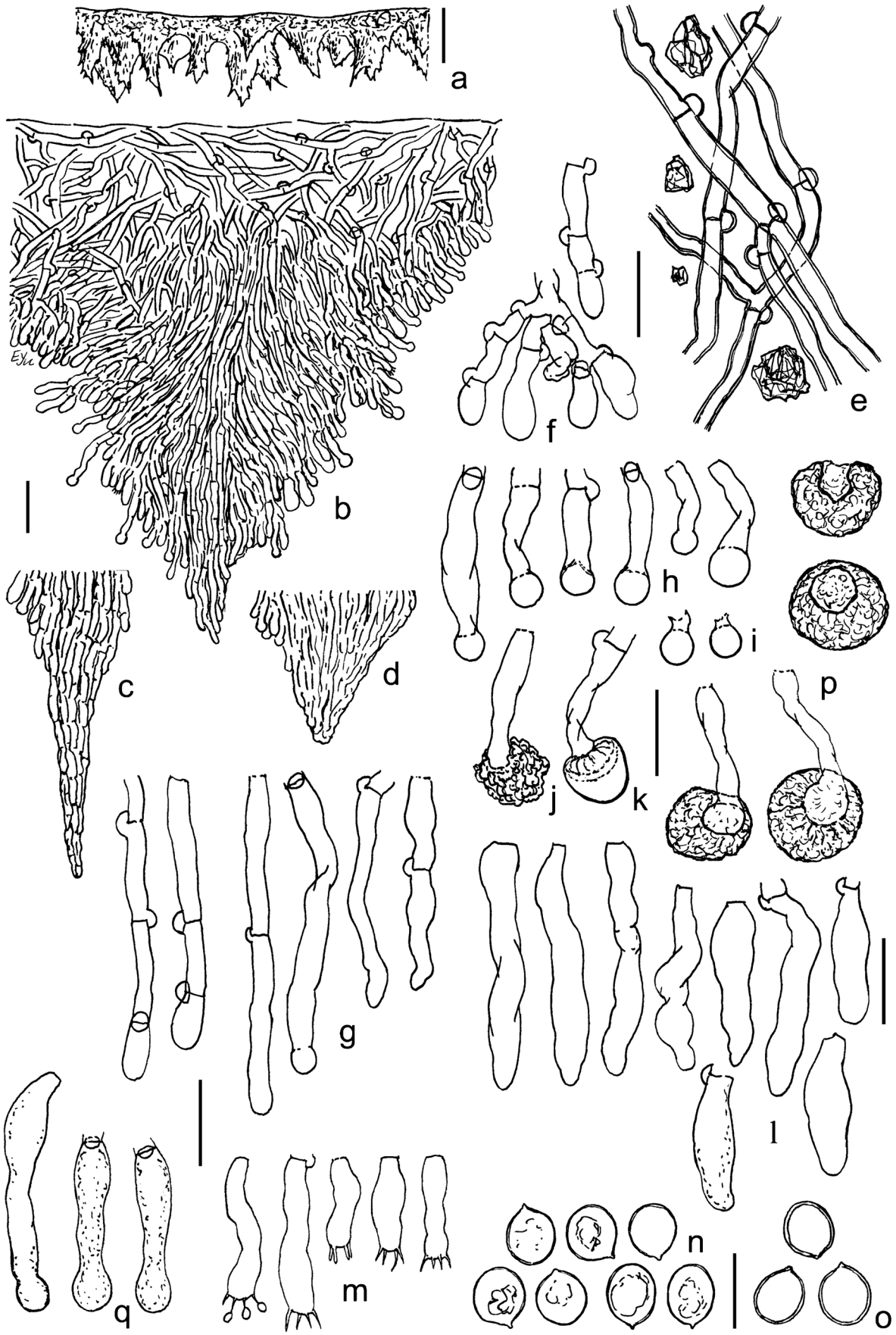
a
b
c
d
e
f
g
h
i
j
k
l
m
n
o
p
q

◂**Fig. 11** Micromorphology of *Xylodon gloeocystidiifer*. Holotype (BLS M-5231): **a**, **b** vertical sections through basidioma; **c**, **d** agglutinated hyphal ends at aculeal apices; **e** subicular hyphae; **f** basidioles and subhymenial hyphae; **g** hyphal ends from aculei; **h** capitate cystidia; **i** broken tips of capitate cystidia; **j**, **k** capitate cystidia with excreted cap; **l** gloeocystidia; **m** basidia; **n**, **o** basidiospores. Paratype (EYu 190720-11 (CFMR)): **p** excreted caps on capitate cystidia and detached from them; **q** gloeocystidia-like capitate elements. **b**–**j**, **l**–**n**, **q** preparations in KOH; **k**, **o** preparations in Mz, **p** preparation in CB. Scale bars = 100 µm for **a**, 20 µm for **b**–**d**, 10 µm for **e**–**m**, **p**, **q**; 5 µm for **n**, **o**

here the single correct name for the species, *X. yunnanensis*. In this case, *H. yunnanensis* is a heterotypic synonym of *X. yunnanensis* (we do not consider it a homonym because of the different generic epithet).

Xylodon yunnanensis **Xue W. Wang & L.W. Zhou**, in Wang, May, Liu & Zhou, Journal of Fungi 7, 478: 67 (2021)

= *Hyphodontia yunnanensis* C.L. Zhao & Y.C. Dai, in Boonmee et al., Fungal Diversity 111: 275 (2021).

Xylodon daweishanensis as insufficiently known taxon

Recently a new species, *Xylodon daweishanensis* C.L. Zhao, was described (Guan et al. 2023), which apparently belongs in our phylogeny to *X. hyphodontinus* s. l. (Figs. 2, 4). This new species is based on five specimens collected from a single locality in Yunnan, China, and the only difference from *X. hyphodontinus*, noted by the authors, is smaller spore size, 3–4 × 2.5–3.5(–4) µm. Our specimen MSK-F 7397 from Taiwan belong to the same subclade as *X. daweishanensis*, but it has slightly bigger spores, 3.5−4.5 × 3.5−4(−4.5) µm. The specimens from other phylogenetically distinct subclades of *X. hyphodontinus* have spores of the same size range as MSK-F 7397, except LIP GG-MAR12-238. The latter possesses spores 3.8−5.4 µm in diameter (G. Gruhn, pers. comm.). Since sequence data from additional genome loci are unavailable for X. *daweishanensis* and *X. hyphodontinus*, we place *X. daweishanensis* amongst insufficiently known taxa.

Discussion

Xylodon lanatus species complex

We have revised here the taxonomy of the *X. lanatus* species complex, which contains species possessing clusters of projecting, encrusted hyphae or hyphoid cystidia. In light of new sequences, this strongly supported clade can be divided into six separate phylospecies (Figs. 2, 3). Two of them, *X. afromontanus* and *X. mantiqueirensis*, are geographically and morphologically distinct from *X. lanatus* s. str., though the morphological differences are not especially pronounced. To clarify the phylogenetic position of *X. lanatus*, and to clarify its morphological differences from other components of the *X. lanatus* complex, we assigned an epitype to *X. lanatus* s. str., following the recommendations for epitypification (Hyde and Zhang 2008).

Earlier, *X. lanatus* s. str. was known from the mainland part of the USA only (Riebesehl et al. 2019). The present study expands the range of this species to Puerto Rico and Ecuador. Thus, the range of *X. lanatus* under the current concept covers temperate coniferous forests (southeast of the USA) and subtropical and tropical moist broadleaf forests (Puerto Rico and Ecuador; Olson et al. 2001), which is not a very common event amongst fungi. We should note, however, that specimens from Puerto Rico and Ecuador form a separate cluster (PP = 1) within the *X. lanatus* clade (Figs. 2, 3). We do not exclude that after adding several genetic loci in phylogenetic reconstruction, these specimens can be classified as a separate species. Thus, we based the morphological description of *X. lanatus* above on specimens from temperate localities only.

Our data expanded the known natural range of *X. echinatus* to the western part of Sunda Archipelago. Earlier the species was known from further north: the protologue of *Hyphodontia echinata* was based on three specimens from Taiwan and one specimen from Yunnan, China (Yurchenko et al. 2013).

Xylodon hyphodontinus species complex

Our ITS phylogeny suggests that specimens identified as *X. hyphodontinus* (Fig. 2) may belong to five phylospecies, based on branch length and branch support. Three of this phylospecies are geographically defined: the first one from mainland China and Taiwan, the second from Kenya, and the third from Panama. However, we observed no significant morphological differences amongst these phylospecies, as well as in our previous study (Riebesehl et al. 2019). There are, for example, less encrusted bunches of cystidia in BLS M-5236 in contrast to LIP GG-MAR15-127 and LIP GG-MAR12-238, but this can be explained as non-hereditary variation. In this case, we observe the phenomenon when microevolution rate, reflected in ITS and 28S sequence changes, is higher than morphological differentiation.

With this broad concept *X. hyphodontinus* has a pantropical distribution: we document here the first finds in Central America (Panama) and Taiwan, and confirmed the occurrence of the species in Ecuador and Cameroon (see list of studied specimens).

Specimens examined for species not presented in the Taxonomy section *Xylodon echinatus* – Taiwan. Chiayi County, Alishan Hsiang, Nanhsi Forest Road, coll. S.H. Wu, J.Y.

Teng, 8 Dec 1994, Wu 9412-34 (TNM F24751, holotype). Indonesia. Java Island, Jawa Tengah (Central Java) Province, Karanganyar, Mt. Lawu, Cemoro Kandang peak trail, about 2270 m a.s.l., secondary (after fire) *Acacia* forest, on naked wood of man-made *Acacia* cf. *decurrens* Willd. stump, leg. O. Miettinen, 22 May 2014, OM 18328 (H 7200350). Malaysia. Borneo Island, Sabah State, near Kota Kinabalu city, on dead corticated wood, leg. U. Frieling, Oct 2017 (KAS-JR31; dupl. in BLS); Sabah State, on dead hardwood, leg. O. Miettinen, 20 Jun 2013, OM 16459 (H 7200689; dupl. SNP 35201).

Xylodon hyphodontinus – Côte d'Ivoire. Forest of Téké north of Abidjan, on cut wood, leg. G. Gilles, 7 Jul 1974, 248 (LY 7377; holotype of *Pteridomyces sphaericosporus*). Cameroon. South Province, near Akok, lowland rainforest reserve, coll. M. Núñez, L. Ryvarden, Dec 1991, No. 31192/LR 7725 (O-F-907725; dupl. H 7004978). Ecuador. Orellana Province, the vicinity of Puerto Francisco de Orellana, 0.4861°S, 76.9500°W, 260 m a.s.l., Amazonian rainforest, on dead rachis of *Musa* sp. leaf, leg. E. Yurchenko, 20 Jul 2019, EYu 190720-68 (BLS M-5236). Panama. Chiriquí Province, Bajo Mono NW of Boquete, southern slopes of Cordillera de Talamanca, 8.8431°N, 82.4750°W, about 1900 m a.s.l., evergreen mountain rainforest, on dead wooden stem, leg. E. Yurchenko, 28 Jul 2019, EYu 190728-2 (MSK-F 11103); *ibid*., on fallen bush stem, leg. E. Yurchenko, 28 Jul 2019, EYu 190728-9 (BLS M-5237). Taiwan. Taipei County, Wulai, Neidong Natural Forest Recreation Area, 24.8333°N, 121.5333°E, 360 m a.s.l., broadleaf montane subtropical forest, on base of dead small stump of angiosperm tree or bush and partly on soil particles, leg. E. Yurchenko, 23 Jun 2011, EYu 110623-23b (MSK-F 7397; dupl. in BLS).

Xylodon pseudolanatus – USA. Tennessee, Sevier, Little River, Jakes Creek Trail, leg. H.H. Burdsall, Jr., 9 Jul 1970 (CFMR HHB-4305); Virginia, Giles Co., Cascades parking lot, leg. H.H. Burdsall, Jr., 2 Aug 1979 (CFMR HHB-10703-Sp); North Carolina, Wake County, W.B. Umstead State Park, middle-aged, lightly burned *Pinus-Acer* forest, on dead wood of uprooted tree of *Acer* (decay stage 2; 12 cm diam.), leg. O. Miettinen, 13 Nov 2013, OM 17556.2 (H 7200690).

Acknowledgements Some DNA extracts and amplicons for this study were obtained thanks to the assistance of Sylvia Heinemann (University of Kassel, Germany), Ann-Christin Brenken, and Henrike Gottfried (Institute for Plant Protection in Horticulture and Urban Green, JKI, Braunschweig, Germany). SEM images were obtained with the kind help of Konrad Wilamowski (Institute of Forest Sciences, Hajnówka, Poland). SEM image of *Xylodon echinatus* holotype (Fig. 7e) was obtained with the assistance of S.K. Hu (Taiwan National Museum of Natural Science, Taichung, R.O.C.). We are grateful to the curators and workers of fungaria, Beatriz Ortiz-Santana (CFMR, USA), Mika Bendiksby (O, Norway), Ewald Langer (KAS, Germany), Yu-Ling Huang (TNM, Taiwan), Blandine Bärtschi (LY, France) and Adriana Gugliotta (SP, Brazil), for providing us *Xylodon* specimens for this research. We thank Leif Ryvarden for opening his herbarium and hosting OM during his stay in Oslo. Two anonymous reviewers are acknowledged for the critical consideration of the MS.

Author contribution Fungal specimens were collected by E. Yurchenko, V. Motato-Vásquez and O. Miettinen. Microscopic examinations of the fungi were done by E. Yurchenko, I. Viner and V. Motato-Vásquez. DNA extraction, amplification and preparation for sequencing were performed by J. Riebesehl, I. Viner and V. Motato-Vásquez. Sequence annotations for GenBank were prepared by J. Riebesehl and I. Viner. Phylogeny reconstructions were performed by J. Riebesehl and O. Miettinen. Photographs from the basidiomata, line drawings, graphic plate with SEM images, and the drafts of the manuscript were prepared by E. Yurchenko. A photograph (Fig. 8a) was done by V. Motato-Vásquez. Final formatting of the manuscript was done by J. Riebesehl and E. Yurchenko. All authors commented on the manuscript.

Funding Open Access funding enabled and organized by Projekt DEAL. The research of E. Yurchenko was financially supported from Polish National Agency for Academic Exchange (NAWA) within the framework of the programme 'Solidarni z Białorusią – Solidarni z naukowcami' (grant BPN/SZN/2021/1/00001, 2022), and from Białystok University of Technology (work No. WZ/WB-INL/2/2021, in 2023).

The research of O. Miettinen and I. Viner was supported by a 3-year research project from the University of Helsinki, and additionally, from Societas pro Fauna et Flora Fennica grant for I. Viner. The research of V. Motato-Vásquez was supported by a PhD grant from Coordenação de Aperfeiçoamento de Nivel Superior (CAPES).

Data availability The DNA sequences generated during the current study are available in NCBI GenBank. Alignments and trees are available as supplementary material.

Declarations

Ethics approval and consent to participate Not applicable.

Consent for publication Not applicable.

Competing interests The authors declare no competing interests.

References

Benson DA, Cavanaugh M, Clark K, Karsch-Mizrachi I, Ostell J et al (2018) GenBank. Nucleic Acids Res 46(D1):D41–D47. https://doi.org/10.1093/nar/gkx1094

Boonmee S, Wanasinghe DN, Calabon MS, Huanraluek N, Chandrasiri SKU et al (2021) Fungal diversity notes 1387–1511: taxonomic and phylogenetic contributions on genera and species of

fungal taxa. Fungal Divers 111:1–335. https://doi.org/10.1007/s13225-021-00489-3
Bunyard BA, Chaichuchote S, Nicholson MS, Royse DJ (1996) Ribosomal DNA analysis for resolution of genotypic classes of *Pleurotus*. Mycol Res 100(2):143–150. https://doi.org/10.1016/S0953-7562(96)80112-2
Chen CC, Wu SH, Chen CY (2017) Three new species of *Hyphodontia* s.l. (*Basidiomycota*) with poroid or raduloid hymenophore. Mycol Prog 16:553–564. https://doi.org/10.1007/s11557-017-1286-0
Cho Y, Kim JS, Dai YC, Gafforov Y, Lim YW (2021) Taxonomic evaluation of *Xylodon* (*Hymenochaetales*, *Basidiomycota*) in Korea and sequence verification of the corresponding species in GenBank. PeerJ 9:e12625. https://doi.org/10.7717/peerj.12625
Fernández-López J, Martín MP, Dueñas M, Telleria MT (2018) Multilocus phylogeny reveals taxonomic misidentification of the *Schizopora paradoxa* (KUC8140) representative genome. MycoKeys 38:121–127. https://doi.org/10.3897/mycokeys.38.28497
Fernández-López J, Telleria MT, Dueñas M, Laguna-Castro M, Schliep K, Martín MP (2020) Linking morphological and molecular sources to disentangle the case of *Xylodon australis*. Sci Rep-UK 10(1):22004. https://doi.org/10.1038/s41598-020-78399-8
Fukami T, Dickie IA, Wilkie PJ, Paulus BC, Park D, Roberts A, Buchanan PK, Allen RB (2010) Assembly history dictates ecosystem functioning: evidence from wood decomposer communities. Ecol Lett 13(6):675–684. https://doi.org/10.1111/j.1461-0248.2010.01465.x
Gardes M, Bruns TD (1993) ITS primers with enhanced specificity for basidiomycetes – application to the identification of mycorrhizae and rusts. Mol Ecol 2(2):113–118. https://doi.org/10.1111/j.1365-294X.1993.tb00005.x
Guan QX, Huang J, Huang J, Zhao CL (2023) Five new species of *Schizoporaceae* (*Basidiomycota*, *Hymenochaetales*) from East Asia. MycoKeys 96:25–56. https://doi.org/10.3897/mycokeys.96.99327
Hjortstam K, Ryvarden L (2007) Studies in corticioid fungi from Venezuela III (*Basidiomycotina*, *Aphyllophorales*). Synopsis Fungorum 23:56–107
Hopple JS, Vilgalys R (1994) Phylogenetic relationships among coprinoid taxa and allies based on data from restriction site mapping of nuclear rDNA. Mycologia 86(1):96–107. https://doi.org/10.1080/00275514.1994.12026378
Hyde KD, Zhang Y (2008) Epitypification: should we epitypify? J Zhejiang Univ-Sc B 9(10):842–846. https://doi.org/10.1631/jzus.B0860004
Katoh K, Rozewicki J, Yamada KD (2019) MAFFT online service: multiple sequence alignment, interactive sequence choice and visualization. Brief Bioinform 20(4):1160–1166. https://doi.org/10.1093/bib/bbx108
Kotiranta H, Saarenoksa R (2000) Three new species of *Hyphodontia* (*Corticiaceae*). Ann Bot Fenn 37:255–278
Kutuzova IA, Kokaeva LY, Pobedinskaya MA, Krutyakov YuA, Skolotneva ES, Chudinova EM, Elansky SN (2017) Resistance of *Helminthosporium solani* strains to selected fungicides applied for tuber treatment. J Plant Pathol 99(3):635–642. https://doi.org/10.4454/jpp.v99i3.3950
Landvik S (1996) *Neolecta*, a fruit-body producing genus of the basal ascomycetes, as shown by SSU and LSU rDNA sequences. Mycol Res 100(2):199–202. https://doi.org/10.1016/S0953-7562(96)80122-5
Larsson KH, Larsson E, Kõljalg U (2004) High phylogenetic diversity among corticioid homobasidiomycetes. Mycol Res 108(9):983–1002. https://doi.org/10.1017/S0953756204000851
Larsson KH, Parmasto E, Fischer M, Langer E, Nakasone KK, Redhead SA (2006) *Hymenochaetales*: a molecular phylogeny for the hymenochaetoid clade. Mycologia 98(6):926–936. https://doi.org/10.3852/mycologia.98.6.926
Luo KY, Chen ZY, Zhao CL (2022) Phylogenetic and taxonomic analysis of three new wood-inhabiting fungi of *Xylodon* (*Basidiomycota*) in a forest ecological system. J Fungi 8(4):405. https://doi.org/10.3390/jof8040405
Luo KY, Qu MH, Zhao CL (2021) Additions to the knowledge of corticioid *Xylodon* (*Schizoporaceae*, *Hymenochaetales*): introducing three new *Xylodon* species from southern China. Diversity 13:581. https://doi.org/10.3390/d13110581
Ma X, Zhao CL (2021) *Xylodon bambusinus* und *X. xinpingensis* spp. nov. (*Hymenochaetales*) from southern China. Phytotaxa 511(3):231–247. phytotaxa.511.3.3
Martin KJ, Rygiewicz PT (2005) Fungal-specific PCR primers developed for analysis of the ITS region of environmental DNA extracts. BMC Microbiol 18(5):28. https://doi.org/10.1186/1471-2180-5-28
Milne I, Lindner D, Bayer M, Husmeier D, McGuire G, Marshall DF, Wright F (2008) TOPALi v2: a rich graphical interface for evolutionary analyses of multiple alignments on HPC clusters and multi-core desktops. Bioinformatics 25(1):126–127. https://doi.org/10.1093/bioinformatics/btn575
Nilsson RH, Tedersoo L, Abarenkov K, Ryberg M, Kristiansson E, Hartmann M, Schoch CL, Nylander JAA, Bergsten J, Porter TM, Jumpponen A, Vaishampayan P, Ovaskainen O, Hallenberg N, Bengtsson-Palme J, Eriksson KM, Larsson KH, Larsson E, Kõljalg U (2012) Five simple guidelines for establishing basic authenticity and reliability of newly generated fungal ITS sequences. MycoKeys 4:37–63. https://doi.org/10.3897/mycokeys.4.3606
O'Donnell K (1993) *Fusarium* and its near relatives. In: Reynolds DR, Taylor JW (eds) The fungal holomorph: mitotic, meiotic and pleomorphic speciation in fungal systematics. CAB International, Wallingford, pp 225–233
Olson DM, Dinerstein E, Wikramanayake ED, Burgess ND, Powell GVN et al (2001) Terrestrial ecoregions of the world: a new map of life on Earth. BioScience 51(11):933–938. https://doi.org/10.1641/0006-3568(2001)051[0933:TEOTWA]2.0.CO;2
Qu MH, Wang DQ, Zhao CL (2022) A phylogenetic and taxonomic study on *Xylodon* (*Hymenochaetales*): focusing on three new *Xylodon* species from Southern China. J Fungi 8:35. https://doi.org/10.3390/jof8010035
Qu MH, Zhao CL (2022) *Xylodon flocculosus* sp. nov. from Yunnan China. Mycotaxon 137(2):189–201. https://doi.org/10.5248/137.189
Rambaut, A. (2018). FigTree v1.4.4. http://tree.bio.ed.ac.uk/software/figtree
Riebesehl J, Langer E (2017) *Hyphodontia* s.l. (*Hymenochaetales*, *Basidiomycota*): 35 new combinations and new keys to all 120 current species. Mycol Prog 16(6):637–666. https://doi.org/10.1007/s11557-017-1299-8
Riebesehl J, Yurchenko E, Nakasone KK, Langer E (2019) Phylogenetic and morphological studies in *Xylodon* (*Hymenochaetales*, *Basidiomycota*) with the addition of four new species. MycoKeys 47:97–137. https://doi.org/10.3897/mycokeys.47.31130
Ronquist F, Teslenko M, van der Mark P, Ayres DL, Darling A et al (2012) MrBayes 3.2: efficient Bayesian phylogenetic inference and model choice across a large model space. Syst Biol 61(3):539–542. https://doi.org/10.1093/sysbio/sys029
Rosenthal LM, Larsson KH, Branco S, Chung JA, Glassman SI, Liao HL, Peay KB, Smith DP, Talbot JM, Taylor JW, Vilgalys R, Bruns TD (2017) Survey of corticioid fungi in North American pinaceous forests reveals hyperdiversity, underpopulated sequence databases, and species that are potentially ectomycorrhizal. Mycologia 109(1):115–127. https://doi.org/10.1080/00275514.2017.1281677
Shi ZW, Wang XW, Zhou LW, Zhao CL (2019) *Xylodon kunmingensis* sp. nov. (*Hymenochaetales*, *Basidiomycot*a) from southern China. Mycoscience 60:184–188. https://doi.org/10.1016/j.myc.2019.02.002

Tamura K, Stecher G, Kumar S (2021) MEGA11: Molecular Evolutionary Genetics Analysis Version 11. Mol Biol Evol 38(7):3022–3027. https://doi.org/10.1093/molbev/msab120

Thiers BM (2023) [continuously updated] Index Herbariorum: a global directory of public herbaria and associated staff. New York Botanical Garden's Virtual Herbarium. http://sweetgum.nybg.org/science/ih

Vilgalys R, Hester M (1990) Rapid genetic identification and mapping of enzymatically amplified ribosomal DNA from several *Cryptococcus* species. J Bacteriol 172(8):4238–4246. https://doi.org/10.1128/jb.172.8.4238-4246.1990

Viner I, Spirin V, Zíbarová L, Larsson KH (2018) Additions to the taxonomy of *Lagarobasidium* and *Xylodon* (*Hymenochaetales*, *Basidiomycota*). MycoKeys 41:65–90. https://doi.org/10.3897/mycokeys.41.28987

Viner I, Bortnikov F, Ryvarden L, Miettinen O (2021) On six African species of *Lyomyces* and *Xylodon*. Fungal Systematics and Evolution 8:163–178. https://doi.org/10.3114/fuse.2021.08.13

Viner I, Spirin V, Larsson KH, Miettinen O (2023) Systematic placement of *Lagarobasidium cymosum* and description of two new species. Mycologia 115(1):122–134. https://doi.org/10.1080/00275514.2022.2146978

Wang XW, May TW, Liu SL, Zhou LW (2021) Towards a natural classification of *Hyphodontia* sensu lato and the trait evolution of basidiocarps within *Hymenochaetales* (*Basidiomycota*). Journal of Fungi 7:478. https://doi.org/10.3390/jof7060478

White TJ, Bruns T, Lee S, Taylor J (1990) Amplification and direct sequencing of fungal ribosomal RNA genes for phylogenetics. In: Innis MA, Gelfand DH, Sninsky JJ, White TJ (eds) PCR protocols: a guide to methods and applications. Academic Press, San Diego, pp 315–322. https://doi.org/10.1016/B978-0-12-372180-8.50042-1

Yurchenko E (2008) Corticioid fungi (*Basidiomycota*) on living wooden plants in Belarus: species inventory and host colonization strategies. Bothanica Lithuanica 14(3):177–189

Yurchenko E, Riebesehl J, Langer E (2017) Clarification of *Lyomyces sambuci* complex with the descriptions of four new species. Mycol Prog 16(9):865–876. https://doi.org/10.1007/s11557-017-1321-1

Yurchenko E, Riebesehl J, Langer E (2020) *Fasciodontia* gen. nov. (*Hymenochaetales*, *Basidiomycota*) and the taxonomic status of *Deviodontia*. Mycol Prog 19(2):171–184. https://doi.org/10.1007/s11557-019-01554-7

Yurchenko E, Wu SH (2014) Three new species of *Hyphodontia* with peg-like hyphal aggregations. Mycol Prog 13(3):533–545. https://doi.org/10.1007/s11557-013-0935-1

Yurchenko E, Xiong HX, Wu SH (2013) Four new species of *Hyphodontia* (*Xylodon* ss. Hjortstam & Ryvarden, *Basidiomycota*) from Taiwan. Nova Hedwigia 96(3–4):545–558. https://doi.org/10.1127/0029-5035/2013/0092

Zhao CL, Cui BK, Dai YC (2014) Morphological and molecular identification of two new species of *Hyphodontia* (*Schizoporaceae*, *Hymenochaetales*) from southern China. Cryptogamie Mycol 35(1):87–97. https://doi.org/10.7872/crym.v35.iss1.2014.87